Current Titles

National Center for Electron Microscopy

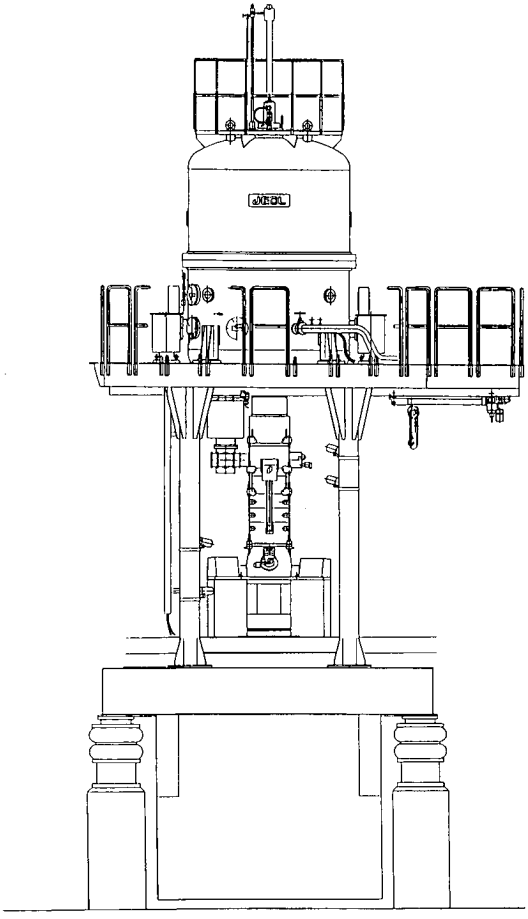

April 2002

Please send a reprint of the paper(s):

Number	First Author	Title (first two words)

Name_____ Date_____

Affiliation _____

Address _____

_____

Please send a reprint of the paper(s):

Number	First Author	Title (first two words)

Name_____ Date_____

Affiliation _____

Address _____

_____

National Center for Electron Microscopy
Lawrence Berkeley National Laboratory
One Cyclotron Road
M/S 72-150
Berkeley, California 94720

National Center for Electron Microscopy
Lawrence Berkeley National Laboratory
One Cyclotron Road
M/S 72-150
Berkeley, California 94720

Current Titles

National Center for Electron Microscopy
Ernest Orlando Lawrence
Berkeley National Laboratory
University of California
Berkeley, California 94720

April 2002

PUB-719 2002

For current information about the NCEM and a
searchable version of publications
visit our website:
http://ncem.lbl.gov

The NCEM is supported by the Director, Office of Science
U.S. Department of Energy
under Contract No. DE-AC03-76SF00098.

This booklet is published for those interested in current research being conducted at the National Center for Electron Microscopy. The NCEM is a DOE-designated national user facility and is available at no charge to qualified researchers. Access is controlled by an external steering committee. Interested researchers may contact Jane Cavlina, Administrator, at 510/486-6036.

Copies of available papers in print may be ordered by their publication number using the enclosed order cards.

Damage Evolution in Dynamic Deformation of Silicon Carbide

C.J. Shih, M.A. Meyers, V.F. Nesterenko and S. J. Chen

Acta Mat. 48, 2399, 2000

Two different hot-pressed silicon carbides, representing two major families of SiC (B-doped and Al-doped SiC) were dynamically deformed, using split Hopkinson bars and rod impact, to study damage evolution. B-doped SiC has a transgranular fracture; whereas, Al-doped SiC has a predominantly intergranular fracture. Fracture mode is independent of strain rate, and SiC exhibiting intergranular fracture has a higher fracture toughness. Fragment size of the SiC is determined by fracture toughness, and SiC has the higher fracture toughness and larger size. Polytype transformation was observed at high impact stress (> 4.5 GPa) during dynamic deformation. Intergranular phases are absent in both SiC. Fracture modes of the SiC depend on microstructural defects; stacking faults and dislocation. Dislocations are not active in the B-dopedSiC; however, dislocation generation and pile-ups are observed in the Al-doped SiC. This dislocation activity is consistent between the simple uni-axial loading (split Hopkinson bar testing) and complicated tri-axial loading with a lateral confinement (rod impact). Two mechanisms are proposed to interpret the fracture modes: dilatant crack and Zener-Stroh cracks. Dilatant cracks are nucleated on the grain boundary, induced by twins (stacking faults) and mismatch in the effective moduli between two adjacent grains and lead to transgranular fracture.

47816 **Novel Joining of Dissimilar Ceramics in the Si_3N_4.Al_2O_3 System Using Polytypoid Functional Gradients**

C. S. Lee, X. F. Zhang and G. Thomas

Acta Mat. 49, 3775-3780, 2001

A unique approach to crack-free joining of heterogeneous ceramics is demonstrated by the use of sialon polytypoids as Functionally Graded Materials (FGM) as defined by the phase diagram in the system, Si_3N_4-Al_2O_3. Polytypoids in the Al_2O_3-Si_3N_4 system offer a path to compatibility for heterogeneous ceramics. This paper describes successful hot press sintering of multilayered FGM's with 20 layers of thickness 500 μm each. Transmission Electron Microscopy was used to identify the polytypoids at the interfaces of different areas of the joint. It has been found that the 15R polytypoid was formed in the Al2O3-contained layers and the 12H polytypoid was formed in the Si3N4-contained layers

49533 **Equilibrium Shape and Interface Roughening of Small Liquid Pb Inclusions in Solid Al**

H. Gabrisch, L. Kjeldgaard, E. Johnson and U. Dahmen

Acta Mat. 49 4259-4269, 2001

The shape of liquid Pb inclusions embedded in a solid Al matrix was investigated at temperatures between 300 and 500°C using in-situ electron microscopy. Inclusion shapes in the size range from a few nanometers to about 150 nanometers were found to depend on size, temperature and thermal history. During isothermal annealing after melting, small inclusions rounded off while larger inclusions remained faceted until the temperature was raised to about 500°C. During subsequent cooling, inclusions refaceted, although less strongly than during heating. The shape hysteresis between heating and cooling cycles was found to be due to the barrier of ledge nucleation necessary to advance the faceted interfaces. It is shown that this kinetic barrier can explain the observed dependence on size and temperature, and that the {111} interface undergoes a roughening transition at about 550°C. The anisotropy of interfacial energy was shown to be significantly smaller than previously reported, and at about 2 %, similar to the anisotropy of the surface energy for fcc metals. From the width of facets on the equilibrium shape, the step energy was determined to be 1.9×10^{-11} J/m at 350°C.

48680 **Imaging of the Crystal Structure of Silicon Nitride at 0.8 Ångstrom Resolution**

A. Ziegler, C. Kisielowski and R.O. Ritchie

Acta Mat. 50, 565-74, 2001

High-resolution transmission electron microscopy is utilized to examine the crystal structure of a silicon nitride ceramic using focus variation methods to achieve sub-ångström resolution at the absolute theoretical information limit of the transmission electron microscope. Specifically, crucial requirements of high instrumental stability, a coherent electron source and optimum imaging conditions have been met by the one-Ångstrom microscope (OÅM) at the National Center for Electron Microscopy in order to obtain a resolution of 0.8 Å. The resulting high-resolution images reveal the individual atom positions of the in-plane projected crystal structure of silicon nitride and permit detailed structural information. The images correspond closely to computed and simulated images of this crystal structure.

General Route to Homogeneous, Mesoporous, Multicomponent Oxides Based on the Thermolytic Transformation of Molecular Precursors in Nonpolar Media

J. W. Kriesel, M. S. Sander and T. Don Tilley

Adv. Mat. 13, 331, 2001

A general route for the synthesis of homogeneous mixed-element oxides, based on the use of block polyalkylene oxide copolymers and single-source molecular precursors, is described. Thermolytic decomposition of the molecular precursors in the presence of an anhydrous solution of the block copolymer (in toluene) led to monolithic gels. The polymeric structure-directing agent was then removed by calcination at 500 °C for 3 h under O2. The generality of this synthetic approach is demonstrated with the molecular precursors Zr[OSi(O*t*Bu)3]4, (EtO)2Ta[OSi(O*t*Bu)3]3, Fe[OSi(O*t*Bu)3]3oTHF and [Al(O*i*Pr)2O2P(O*t*Bu)2]4, which have been converted to the corresponding mesostructured materials ZrO2o4SiO2, Ta2O5o6SiO2, Fe2O3o6SiO2 and AlPO4 (denoted UCB1-ZrSi, UCB1-TaSi, UCB1-FeSi, UCB1-AlP, respectively). These mesostructured materials, characterized by TEM, XRD, N2 porosimetry, EDX and NMR spectroscopy, exhibit wormhole-like pore structures, high surface areas and narrow pore size distributions.

Characterization of Free-Standing Hydride Vapor Phase Epitaxy GaN

J. Jasinski, W. Swider, Z. Liliental-Weber, P. Visconti, K. M. Jones, M. A. Reshchikov, F. Yun, H. Morkoç, S. S. Park et al

Appl. Phys. Lett. 78, 2297, 2001

A free-standing GaN template grown by hydride vapor phase epitaxy has been characterized by transmission electron microscopy (TEM). The TEM investigation was augmented by X-ray diffraction, defect delineation etching process followed by imaging with atomic force microscopy and variable temperature photoluminescence. The density of dislocations near the N face was determined to be, in order, 3*107, 4*107, and about 1*107 cm-2 by cross-sectional TEM, plan-view TEM, and a defect revealing etch, respectively. The same methods on the Ga face revealed the defect concentration to be, in order, less than 1*107 cm-2 by plan-view TEM, less than 5*106 cm-2 by cross-sectional TEM, and 5*105 cm-2 by defect revealing hot H3PO4 acid, respectively. The full width at half maximum of the symmetric (0002) X-ray diffraction peak was 69 and 160 arc sec for the Ga and N faces, respectively. That for the asymmetric (10104) peak was 103 and 140 arc sec for Ga and N faces, respectively. The donor bound exciton linewidth was about 1 meV each at 10 K, and a green band centered at about 2.44 eV was observed.

Microstructural Evidence on Electrical Properties of Ta/Ti/Al and Ti/Ta/Al Ohmic Contacts to n-AlGaN/GaN

S.-H. Lim, J. Washburn, Z. Liliental-Weber and D. Qiao

Appl. Phys. Lett. 78, 3797, 2001

Electrical properties and microstructures of Ta/Ti/Al and Ti/Ta/Al contacts to n-AlGaN/GaN heterostructure field-effect transistor structures were investigated using the transmission line method and transmission electron microscopy. The specific resistivity (5.3*10-7 Wcm2) of Ta/Ti/Al contacts is much lower than that (5.1*10-4 Wcm2) of Ti/Ta/Al contacts, for the same heterostructure and similar metallization. The contact resistivity was found to depend on the thickness of the AlGaN layer, interfacial phase, and interface roughness. The formation of interfacial phases by solid-state reactions with the metal layer during annealing appears to be essential for ohmic behavior on n-III-nitrides suggesting a tunneling contact mechanism.

Quantitative in-situ Nanoindentation in an Electron Microscope

A.M. Minor, J.W. Morris Jr. and E.A. Stach

Appl. Phys. Lett. 79, 11, 1625-27, 2001

We report the development of a method for quantitative, in situ nanoindentation in an electron microscope and its application to study the onset of deformation during the nanoindentation of aluminum films. The force–displacement curve developed shows the characteristic "staircase" instability at the onset of plastic deformation. This instability corresponds to the first appearance of dislocations in a previously defect-free grain. Plastic deformation proceeds through the formation and propagation of prismatic loops punched into the material, and half loops that emanate from the sample surface. These results represent the first real time observations of the discrete microstructural events that occur during nanoindentation

Magnetic Imaging of Ion-Irradiation Patterned Co/Pt Multilayers Using Complementary Electron and Photon Probes

G.J. Kusinski, K.M. Krishnan, G. Thomas, G. Denbeaux, D. Weller, C. Rettner and B.D. Terris

Appl. Phys. Lett. 79, 14, 2211, 2001

The three-dimensional magnetic structure and reversal mechanism of patterned Co/Pt multilayers, were imaged using complementary Lorentz transmission electron microscopy (LTEM) (in-plane component) and magnetic transmission x-ray microscopy (M-TXM) (perpendicular magnetization). The Co/Pt films with perpendicular anisotropy were patterned by ion irradiation through a stencil mask to produce in-plane magnetization in the irradiated regions. The boundaries of the patterns, defined by the transition from out-of-plane to in-plane magnetization, were found to be determined by the stencil mask, whilst the scale of the magnetic reversal by the physical microstructure. The nucleation fields were substantially reduced to ~50-100 Oe for the in-plane regions and ~1 kOe for the perpendicular regions, comparing to 4.5 kOe for the as-grown film. The perpendicular reversals were found to always originate at the pattern boundaries.

Rapid Thermal Annealing of InAs/GaAs Quantum Dots Under a GaAs Proximity Cap

A. Babinski, J. Jasinski, R. Bozek, A. Szepielow and J. M. Baranowski

Appl. Phys. Lett. 79, 2576, 2001

The effect of postgrowth rapid thermal annealing (RTA) on GaAs proximity-capped structures with self-assembled InAs/GaAs quantum dots (QDs) is investigated using transmission electron microscopy (TEM) and photoluminescence (PL). As can be seen from the TEM images, QDs increase their lateral sizes with increasing annealing temperature (up to 700 oC). QDs cannot be distinguished after RTA at temperature 800 oC or higher, and substantial thickening of the wetting layer can be seen instead. The main PL peak blueshifts as a result of RTA. We propose that in the as-grown sample as well, as in samples annealed at temperatures up to 700 oC, the peak is due to the QDs. After RTA at 800 oC and higher the PL peak is due to a modified wetting layer. Relatively fast dissolution of QDs is explained in terms of strain-induced lateral Ga/In interdiffusion. It is proposed that such a process may be of importance in proximity-capped RTA, when no group-III vacancy formation takes place at the sample/capping interface.

47483 **Enhancement of Dislocation Velocities by Stress Assisted Kink Nucleation at the Native Oxide/ SiGe Interface**

E.A. Stach and R. Hull

Appl. Phys. Lett. 79, 3, 335-7, 2001

Experiments have shown that the presence of a thin native oxide layer on the surface of a strained SiGe epilayer causes an order of magnitude increase in dislocation velocities during annealing over those observed in atomically clean samples and during crystal growth. This behavior is explained herein by stress-assisted dislocation kink nucleation at the oxide / epilayer interface. Finite element models are used to estimate the magnitude of stress local to steps at this interface due to both intrinsic and thermal expansion stresses, and dislocation theory is used to determine the resulting increase in single kink nucleation.

Influence of Microstructure on Electrical Properties of Diluted GaNxAs1-x Formed by Nitrogen Implantation

J. Jasinski, K. M. Yu, W. Walukiewicz, J. Washburn and Z. Liliental-Weber

Appl. Phys. Lett. 79, 931, 2001

Structural studies of GaAs implanted with N or coimplanted with other elements showed that, in addition to typical postimplant defects, small voids were present in the implanted region in such materials. Comparison of the microstructure found in these layers with electrical results indicates that these voids are responsible for the low activation efficiency of N implanted into GaAs. The results show that the N-induced enhancement of the donor activation efficiency can be achieved only in a void-free region of the implanted sample.

48681 **Mechanism of Fatigue in Micron-Scale Films of Polycrystalline Silicon for Microelectromechanical Systems**

C. L. Muhlstein, E. A. Stach and R. O. Ritchie

Appl. Phys. Lett. 80, 9,1532, 2002

Reported nearly a decade ago, cyclic fatigue in silicon thin films has remained a mystery. Silicon does not display the room-temperature platisicity or extrinsic toughening mechanisms necessary to cause fatigue in either ductile (e.g. metals) or brittle (e.g. ceramics and ordered intermetallics) materials. This letter presents experimental evidence for the cyclic fatigue of silicon via a conceptually different mechanism termed reaction-layer fatigue. Based on mechanical testing, electron microscopy and self-assembled monolayers, we present direct observation of fatigue-crack initiation in polycrystalline silicon, the mechanism of crack initiation and a method for altering fatigue damage accumulation.

Lorentz Transmission Electron Microscopy Investigation of Magnetically Patterned Co/Pt Multilayers

G.J. Kusinski, K.M. Krishnan, D. Weller, B.D. Terris, L. Folks, A.J. Kellock, J.E.E. Baglin, and G. Thomas

Beyond 2000, NATO Sci., ed. G. Hadjipanayis, Kluwer, 41, 157, 2001

The switching behavior of magnetic patterns prepared by ion irradiation was investigated. Co/Pt multilayers with perpendicular anisotropy and large out-of-plane coercivities 5-6 kOe were grown on electron transparent SiN windows. Regularly spaced 1 micron sized regions, were magnetically pattered via ion beam irradiation through a stencil mask. Lorentz TEM was used to observe in-situ magnetization reversal processes of irradiated regions under well-defined applied magnetic fields. When the in-plane field was increased, domain wall motion was observed, resulting in the alignment of the patterns with the direction of the applied field. The switching mechanism of the in-plane patterns was by domain wall motion.

50064 **Physical and Electrochemical Characterization of Bimetallic Nanoparticle Electrocatalysts**

N. Markovic, V. Radmilovic and P. Ross, Jr.

Catal & Electrocatal at Nanoparticle Surf. M. Dekker Pub., 2002, In Press

We review studies, primarily from our laboratory, of Pt and Pt bimetallic nanoparticle electrocatalysts for the oxygen reduction reaction, and the electrochemical oxidation of H2 and H2/CO mixtures in aqueous electrolytes at 274-333 K. We focus on the study of both the structure sensitivity of the reactions as gleaned from studies for the bulk (bi)metallic surfaces, and the resultant crystallite size effect expected or observed when the catalyst is of nano-scale dimension. Physical characterization of the nanoparticles by high resolution transmission electron microscopy techniques is shown to be an essential tool for these studies. Comparison with well-characterized model surfaces has revealed only a few "nanoparticle anomalies", although the number of bimetallics studies in this manner is still relatively small. It may be that surface segregation thermodynamics unique to nanoparticles can explain some of these anomalies in a consistent manner.

Block Copolymer Assisted Synthesis of Mesoporous, Multicomponent Oxides by Non-hydrolytic, Thermolytic Decomposition of Molecular Precursors in Nonpolar Media

J. W. Kriesel, M. S. Sander and T. Don Tilley

Chem. Mat. 13, 3554, 2001

A general route for the synthesis of homogeneous mixed-element oxides, based on the use of block polyalkylene oxide copolymers and single-source molecular precursors, is described. Thermolytic decomposition of the molecular precursors in the presence of an anhydrous solution of the block copolymer (in toluene) led to monolithic gels. The polymeric structure-directing agent was then removed by calcination at 500 °C for 3 h under O2. The generality of this synthetic approach is demonstrated with the molecular precursors Zr[OSi(O*t*Bu)3]4, (EtO)2Ta[OSi(O*t*Bu)3]3, Fe[OSi(O*t*Bu)3]3oTHF and [Al(O*i*Pr)2O2P(O*t*Bu)2]4, which have been converted to the corresponding mesostructured materials ZrO2o4SiO2, Ta2O5o6SiO2, Fe2O3o6SiO2 and AlPO4 (denoted UCB1-ZrSi, UCB1-TaSi, UCB1-FeSi, UCB1-AlP, respectively). These mesostructured materials, characterized by TEM, XRD, N2 porosimetry, EDX and NMR spectroscopy, exhibit wormhole-like pore structures, high surface areas and narrow pore size distributions.

Selective Area Growth and Characterization of AlGaN/GaN Heterojunction Bipolar Transistors by Metalorganic Chemical Vapor Deposition

B.S. Shelton, D.J.H. Lambert, Jian Jang Huang; M.M. Wong, U. Chowdhury, Ting Gang Zhu; H.K. Kwon, et al

IEEE Transactions on Electron Devices 48, 490, 2001

The selective area growth (SAG) and properties of AlGaN/GaN heterojunction bipolar transistors (HBTs) grown by low-pressure metalorganic chemical vapor deposition (MOCVD) are described and analyzed. Transistors based on group III-nitride material are attractive for high-power and high-temperature applications. Much work has been focused on improving p-type material, as well as heterojunction interfaces. However, there have been very few reports on HBTs operating at room temperature, At this time, current gains for nitride-based HBTs have been limited to ~10. Selective area regrowth was applied to the growth of AlGaN/GaN HBTs to analyze its potential advantages as compared to more traditional growth techniques in order to realize improved electrical performance of the devices.

A Full Field Transmission X-ray Microscope as a tool for High-Resolution Magnetic Imaging

G. Denbeaux, P. Fischer, G. Kusinski, M. Le Gros, A. Pearson and D. Attwood

IEEE Transactions on Magnetics 37, 4, 2764, 2001

The XM-1 soft x-ray microscope, located at the Advanced Light Source at Lawrence Berkeley National Laboratory has recently been established as a tool for high-resolution imaging of magnetic domains. It is a "conventional" full field transmission microscope which is able to achieve a resolution of 25 nm by using high-precision zone plates. It uses off-axis bend magnet radiation to illuminate samples with elliptically polarized light. When the illumination energy is tuned to absorption edges of specific elements, it can be used as an element-specific probe of magnetism on a 25 nm scale with a contrast provided by magnetic circular dichroism. The illumination energy can be tuned between 250-850 eV. This allows imaging of specific elements including chromium, iron and cobalt. The spectral resolution has been shown to be E/_E = 500-700. This spectral resolution allows a high sensitivity so that magnetization has been imaged within layers as thin as 3 nm. Since this is a photon based magnetic microscopy, fields can be applied to the sample even during imaging without affecting the spatial resolution. The current system can apply in-plane or out-of-plane fields approaching 1 kOe. We expect to upgrade this shortly to allow fields in excess of 2 kOe on the sample during imaging.

Evolution of Microstructure, Microchemistry and Coercivity in 2:17 Type Sm-Co Magnets with Heat Treatment

Y. Zhang, W. Tang, G. Hadjipanayis, C. Chen, C. Nelson and K. Krishnan

IEEE Transactions on Magnetics 37, 4 , July 2001

A systematic study has been undertaken to understand the evolution of microstructure, microchemistry, and coercivity of sintered Sm(CobalCu0.06Fe0.015Zr0.027)6.4 magnets with heat treatment using magnetometry, transmission electron microscopy, Lorentz microscopy, and nanoprobe chemical analysis. In general, the homogenized and quenched Sm(CobalCu0.06Fe0.015Zr0.027)6.4 magnets have a featureless microstructure with the 2:17 hexagonal structure. During isothermal aging at 700-850°C, the 1:5 nuclei precipitate and then coalesce and start forming the cellular structure with 2:17 rhombohedral cells surrounded by 1:5 hexagonal cell boundaries. Uniform cellular sand lamellar structures are formed after 2 hours of isothermal aging, and both the cell size and density of lamella phase slightly increase with longer aging. Nanoprobe chemical analysis shows that the Cu content in 1:5 cell boundaries increases during the slow cooling to lower temperatures, reaching a maximum value around 500°C, which is consistent with the development of coercivity. Also the Cu content in the triple cell boundary junctions is twice as much as the amount at the regular cell boundaries regardless of cell size and boundary width. Lorentz microscopy indicates that the triple cell boundary junctions may play a major role in domain wall pinning.

49802 **Electron Microscopy of Nanocrystals Inside Microcrystals**

U. Dahmen, E. Johnson, S.Q. Xiao and S. Hinderberger

Inst. Phys. Conf. Ser. 168, M. Aindow and C.J. Kiely, eds. IOP, 1-8, 2001

We present a summary of recent work on nanocrystalline inclusions embedded in a solid matrix. The effects of elastic constraints, crystallographic symmetry, shape and size are illustrated with two specific examples of inclusions in binary Al alloys. Ge precipitates in dispersion hardening Al-Ge based alloys are shown to be controlled by internal twinning. By comparison, Pb inclusions in binary Al-Pb alloys are free of twins and other defects, and exhibit behaviour that depends strongly on size, shape and interface structure.

49803 **HREM Analysis of Σ3 {112} Boundaries in Gold Bicrystal Films**

C.J.D. Hetherington, U.Dahmen, R. Kilaas, A.I. Kirkland, R.R. Meyer and D.L. Medlin

Inst. Phys. Conf. Ser. 168, M. Aindow and C.J. Kiely, eds., IOP, 51-62, 2001

Gold bicrystal films, with foil normal along <111>, have been observed in the Stuttgart JEOL ARM1250 and Oxford JEOL 3000F microscopes. Phase and modulus images of the Σ3{112} boundaries were reconstructed, images were simulated using models, and the arrangement of facets was considered.

50066 **Evolution of Microstructure and Defect Structure in L_{10}-Ordered Manganese Aluminide Permanent Magnet Alloys**

C. Yanar, V. Radmilovic, W.A. Soffa and J.M. Wiezorek

Intermetallics 9, 949-54, 2001

Defects produced in massively transformed L10-ordered τ– MnAl have been characterized by detailed TEM studies. The defect population in massive τ– MnAl comprises arrays of overlapping octahedral stacking faults, {111}-conjugated microtwins, thermal antiphase boundaries and dislocations. The genesis of these defects has been attributed to atomic attachment faulting on {111}-and {020}-type facets of the essentially incoherent growth interface between the parent and product phases. The features of the defect genesis in τ– MnAl are discussed with respect to the role of atomic level processes at solid-state transformation interfaces in general and growth interfaces in massively transforming materials systems in particular.

Ion Induced Magnetization Reorientation in Co/Pt Multilayers for Patterned Media

D. Weller, J.E.E. Baglin, A.J. Kellock , K.A. Hannibal, M.F. Toney, G. Kusinski, S. Lang, L. Folks, M.E. Best and B.D. Terris

J. Appl. Phys. 87, 5768, 2000

Co/Pt multilayer films with perpendicular magnetic anisotropy and large out-of-plane coercivities of 3.9 - 8.5 kOe have been found to undergo a spin reorientation transition from out-of-plane to in-plane upon irradiation with 700 keV nitrogen ions. X-ray reflectivity experiments show that the multilayer structure gets progressively disrupted with increasing ion dose, providing direct evidence for local atomic displacements at the Co/Pt interfaces. This effectively destroys the magnetic interface anisotropy, which was varied by about a factor of two, between KS0.4 erg/cm2 and KS0.85 erg/cm2 for two particular films. The dose required to initiate spin-reorientation, 6?1014 N+/cm2 and 1.51015 N+/cm2, respectively, scales with KS. It is roughly equal to the number of Co interface atoms per unit interface area contributing to KS.

46725 **Domain Structures and Spin-Reorientation Transitions in C-Axis Oriented Co-Cr Thin Films**

G. Kusinski, K.M. Krishnan, G. Thomas and E.C. Nelson

J. Appl. Phys. 87, 6376, 2000

Highly c-axis oriented $Co_{95}Cr_5$ films with perpendicular anisotropy were grown epitaxially on Si (111), using a Ag seed layer, by physical vapor deposition. Films were characterized by x-ray diffraction, transmission electron microscopy (TEM), selected area electron diffraction (SAD), and Lorentz microscopy in a TEM. The following epitaxial relationship was confirmed: (111)Si || (111)Ag || (0001)CoCr ; . Magnetic domain structures of these films were observed, as a function of thickness, t, in the range 200Å < t < 700Å using a wedge-shaped sample, and temperature-dependent measurements were carried out by *in-situ* resistance heating. Below a critical thickness, tc*300Å, the magnetization was found to be in-plane of the film, and above, tc a regular, stripe-like domain pattern with a significant perpendicular component was observed. The spin reorientation transition of these stripe domains, to a fully in-plane magnetization, with decreasing values of magnetocrystalline anisotropy constant, Ku, were studied dynamically by observing the domains as a function of temperature by *in-situ* heating up to 350°C. The critical transition thickness, tc, which is a function of Ku and the magnetostatic energy, was found to increase with increasing temperature. The stripe-domain period, L observed at room temperature was found to increased gradually with thickness; L=90nm at t=300Å, and L=110nm at t=700Å.

50149 **Exchange Biasing and Interface Structure in MnNi/Fe(Mo) Bilayers**

N. Cheng, K.M. Krishnan, R.F.C. Farrrow, A. Young, E. Girt, R. F. Marks, A. Kellock, and C.H.A. Huan

J. Appl. Phys. 87, 6647, 2000

The role of magnetic, structural and chemical roughness on the origin of exchange biasing in polycrystalline Mn52Ni48/Fe92(Mo8) bilayers has been investigated by (XMCD), (VSM) and (TEM). Three bilayer samples of MnNi(22nm)/Fe(Mo)(6nm) were grown by molecular beam epitaxy under ultrahigh vacuum conditions with the MnNilayer at temperatures of 200*C, 250*C and 300*C. The exchange bias, He was observed to be the largest for the 250*C growth sample. The angular dependence of He can be well modeled in terms of a cosine series with odd terms confirming the unidirectional nature of the anisotropy energy. However, the coefficients are different for the three samples indicating different microscopic magnetic interactions at the interface. XMCD measurements showed no magnetic moment for Mn and Ni but showed systematic variations of the Fe moment, i.e. a decrease in Fe moment with increase in He was observed. We have interpreted this decrease in Fe moment in terms of antiferromagnetic (AF) ordering of Fe at the interface with the extent of the AF ordering being related to the magnitude of the exchange. Thus, for samples grown at 250*C, it is found that at least about 4MLs of Fe appear to be AF. Preliminary energy-filtered imaging of cross-section samples shows that the Fe layer is chemically rough suggesting that the decrease in moment may arise from the intermixing of Fe with the MnNi layer.

Structural and Magnetic Properties of High Coercivity Co/Pt Multilayers

D. Weller, L. Folks, M. Best, E.F. Fullerton, B.D. Terris, G.J. Kusinski, K.M. Krishnan, G. Thomas

J. Appl. Phys. 89, 11, 7525, 2001

10x(t nm Co / 1 nm Pt1) multilayer films (0.2<t<2 nm) with perpendicular anisotropy and room temperature coercivities larger 10,000 Oe are fabricated using electron beam evaporation at elevated substrate temperature onto a 20nm/40nmSiNx/Si(001) seed structure. Hysteresis studies indicate a transition from pinning dominated magnetization reversal for films grown at lower substrate temperatures (RT – 250C) to nucleation dominated behavior for films grown above about 250C. This is particularly evident from initial magnetization curve studies. Magnetic force microscopy studies for this series corroborate this conclusion. High resolution cross sectional TEM studies, with elemental analysis of the highest coercivity films show first of all evidence for columnar multilayer grains with sharp interfaces extending throughout the overall thickness of the films. Second, evidence for Pt enrichment at the column boundaries is found, which is expected to give rise to some exchange decoupling of adjacent grains and therefore explains the high coercivities. Typical perpendicular anisotropy values, normalized to the total volume, are Ku~9x106 erg/cc. The interesting observation is that for growth temperatures up to about 350C, there is little evidence from either X-TEM or X-ray diffraction studies of interfacial intermixing in these structures.

Ta-based Interface Ohmic Contacts to AlGaN/GaN Heterostructures

I. D. Qiao, L. Jia, L.S. Yu, P.M. Asbeck, S.S. Lau, S.-H. Lim, Z. Liliental-Weber, T.E. Haynes and J.B. Barner

J. Appl. Phys. 89, 5543, 2001

Al/Ti based metallization is commonly used for ohmic contacts to n-GaN and related compounds. We have previously reported an ohmic contact scheme specially designed for AlGaN/GaN heterostructure field-effect transistors (HFETs). This scheme, referred to as the "advancing interface" contact, takes advantage of the interfacial reactions between the metal layers and the AlGaN barrier layer in the HFET structure. These reactions consume a portion of the barrier, thus facilitating carrier tunneling from the source/drain regions to the channel region. The advancing interface approach has led to consistently low contact resistance on Al0.25Ga0.75 N/GaN HFETs. There are two drawbacks of the Al/Ti based advancing interface scheme, (i) it requires a capping layer for the ohmic formation annealing since Ti is too reactive and is easily oxidized when annealing is performed in pure N2 or even in forming gas, and (ii) the atomic number of Al and that of Ti are too low to yield efficient backscattered electron emission for e-beam lithographic alignment purposes. In this work, we investigated a Ta based advancing interface contact scheme for the HFET structures. We found that the presence of Ta in this ohmic scheme leads to (1) a specific contact resistivity as low as 5*10-7 Wcm2, (2) efficient electron emission for e-beam lithographic and (3) elimination of the capping layer for the ohmic annealing.

Microstructure of Laterally Overgrown GaN Layers

Z. Liliental-Weber and D. Cherns

J. Appl. Phys. 89, 7833, 2001

Transmission electron microscopy study of plan-view and cross-section samples of epitaxial laterally overgrown (ELOG) GaN samples is described. Two types of dislocation with the same type of Burgers vector but different line direction have been observed. It is shown that threading edge dislocations bend to form dislocation segments in the c plane as a result of shear stresses developed in the wing material along the stripe direction. It is shown that migration of these dislocations involves both glide and climb. Propagation of threading parts over the wing area is an indication of high density of point defects present in the wing areas on the ELOG samples. This finding might shed light on the optical properties of such samples.

47361 **Microstructural Properties of (Ba, Sr) TiO_3 Films Fabricated From $BaF_2/SrF_2/TiO_2$ Amorphous Multilayers Using the Combinatorial Precursor Method**

I. Takeuchi, K.Chang, R. P. Sharma, L. Bendersky, H. Chang, X. D. Xiang, E.A. Stach and C.Y. Song

J. Appl. Phys. 90, 5, 2474-8, 2001

We have investigated the microstructure of (Ba,Sr)TiO3 films fabricated from BaF2/SrF2/TiO2 amorphous multilayers. Rutherford backscattering spectroscopy and x-ray diffraction studies show that a controlled thermal treatment can interdiffuse the multilayers so as to create predominantly single-phase epitaxial (Ba,Sr)TiO3 films. High resolution cross-sectional transmission electron microscopy investigation of the processed films shows that they consist of large epitaxial grains of (Ba,Sr)TiO3 with atomically sharp interfaces with the LaAlO3 substrates. In addition, we have identified regions where polycrystalline and amorphous phases exist in small pockets in the film matrix. The results here indicate that the combinatorial thin-film synthesis using precursors can produce (Ba,Sr)TiO3 films in combinatorial libraries which exhibit properties similar to those films made by conventional techniques.

Temperature and Ion Irradiation Dependence of Magnetic Domains and Microstructure in Co/Pt Multilayers

G.J. Kusinski, G. Thomas, G. Denbeaux, K.M. Krishnan and B.D. Terris

J. Appl. Phys. 91, 10, 2002

Microstructure and magnetic properties of Co/Pt multilayers with perpendicular anisotropy were studied as a function of growth temperature (TG) and ion irradiation. With increased TG, larger columnar grain size and an improved <111> texture were observed. Up to a critical temperature (Tcrit), a monotonic increase in coercivity (*HC*) with TG was measured, followed by a decrease in *HC* with further increase in TG. Magnetic domains of films grown below Tcrit were irregular, with their sub-micron size decreasing gradually with increasing TG. Films grown at 390oC > Tcrit had fine domains on the sub-100 nm length scale. Both *HC* and domain size were reduced after the multilayers were exposed.

Mechanisms of Dislocation Reduction in GaN Using an Intermediate Temperature Interlayer

E.D. Bourret-Courchesne, K.M. Yu, M. Benamara, Z. Liliental-Weber and J. Washburn

J. Elect. Mat. 30, 1417, 2001

A dramatic reduction of the dislocation density in GaN was obtained by insertion of a single thin interlayer grown at an intermediate temperature (IT-IL) after the initial growth at high temperature. A description of the growth process is presented with characterization results aimed at understanding the mechanisms of reduction in dislocation density. A large percentage of the threading dislocations present in the first GaN epilayer are found to bend near the interlayer and do not propagate into the top layer which grows at higher temperature in a lateral growth mode. TEM studies show that the mechanisms of dislocation reduction are identical to those described for the epitaxial lateral overgrowth process, however a notable difference is the absence of coalescence boundaries.

Relaxation of InGaN Thin Layers Observed by X-Ray and Transmission Electron Microscopy Studies

Z. Liliental-Weber, M. Benamara, J. Washburn, J.Z. Domagala, J. Bak-Misiuk, E.L. Piner, J.C. Roberts and S.M. Bedair

J. Elect. Mat. 30, 439, 2001

Double-crystal and triple-axis X-ray diffractometry and transmission electron microscopy are used to characterize the microstructure, strain, and composition of InGaN layers grown on GaN by metalorganic chemical vapor deposition (MOCVD). Three different samples with increasing In concentration have been studied, all grown on GaN deposited on sapphire either with GaN or AlN buffer layers. It was found that InGaN layers with nominal 28% and 40% InN content consist of two sub-layers; the first sub-layer is pseudomorphic with the underlying GaN with lower In content than nominal. The top sub-layer is fully relaxed with a high density of planar defects and In content close to the nominal value. This is in contrast to a common assumption applied to InGaN quantum wells that 'quantum-dot like areas' are formed with different In content. The sample with the nominal indium concentration of 45% does not exhibit any intermediate strained layer, is fully relaxed and the In concentration (43.8%) agrees well with the nominal value.

49809 Nanoscale Lead-Tin Inclusions in Aluminum

E. Johnson, A. Johansen, C. Nelson and U. Dahmen

J. Elect. Mic. 51, S201-09, 2002

Nanoscale lead-tin alloy inclusions have been made by sequential ion implantation of lead and tin in aluminum targets at 150 and 200°C. The alloy inclusions with sizes in the range from 2 to 20 nm form spontaneously during the ion implantation independent of whether lead or tin is implanted first. Alloys with nominal compositions of Pb:Sn equal to 1:1 and 1:3 respectively have inclusion microstructures consisting of segments of a lead-rich fcc phase and a tin-rich tetragonal phase attached to each other along internal interfaces that are often close to (111)fcc. The overall morphology of the inclusions is cuboctahedral-like and most of the inclusions are bicrystalline. Some inclusions, however, have multicrystalline morphology where one or two slabs of lead are attached between two segments of tin or vice versa, resembling a lamellar eutectic structure of nanoscale dimensions. The lead-rich fcc phase grows in parallel cube alignment with the matrix while the orientation relationship of the tin-rich phase varies. Many inclusions have the {111}Pb planes parallel to the {100}Sn planes and in this common plane both the <001>Sn and <011>Sn directions have been found to be parallel to <110>Al. Nanoprobe EDX analysis on the two-phase inclusions with sizes in the range from 10 to 20 nm shows that both phases are supersaturated, and their concentrations are considerably larger than given by the phase diagram around 100°C where equilibrium can still be attained by diffusion.

Microstructure Stability and Room Temperature Mechanical Properties of the Nextel 720 Fibre

F. Deleglise, M.H. Berger, D. Jeulin and A.R. Bunsell

J. Euro. Ceramic Soc. 21, 569-80, 2001

The microstructure and tensile properties of the as-received and heat-treated Nextel 720 fibre have been studied. During its fabrication the Nextel 720 fibre is pyrolysed at a temperature lower than 1400°C for a very short time which does not allow the microstructure to be stabilised. A pseudo-tetragonal metastable alumina rich mullite is formed which crystallises in the form of mosaic grains containing low angle boundaries. These mosaic grains enclose some rounded and elongated α-alumina grains. The evolution of the mullite to the stable orthorhombic symmetry is seen from 1200°C for post heat treatments lasting several hours. For longer heat treatments at 1200°C or at 1300°C and higher temperatures, the mosaic grains begin to recrystallise into single grains and the alumina rejected from the mullite contributes to the growth of elongated α-alumina grains which suggests diffusion through an intergranular liquid silicate phase. At 1400°C theo mullite has the 3:2 composition and after 24 hours the growth of the elongated α-alumina grains leads to a reduction of the room temperature tensile strengths. The α-alumina creation coupled to the phase transformation and dissolution of mullite leads to an increase of the Young's modulus after heat treatments from 1200°C.

47681 **Nitrogen Effects on Crystallization Kinetics of Amorphous TiOxNy Thin Films**

K. Hukari, R. Dannenberg and E.A. Stach

J. Mater. Res. 17, 3, 2002

The crystallization behavior of amorphous TiOxNy (x>>y) thin films was investigated by in-situ transmission electron microscopy.The Johnson-Mehl-Avrami-Kozolog (JMAK) theory is used to determine the Avrami exponent, activation energy, and the phase velocity pre-exponent. Addition of nitrogen inhibits diffusion, increasing the nucleation temperature, while decreasing the growth activation energy. Kinetic variables extracted from individual crystallites are compared to JMAK analysis of the fraction transformed and a change of 6% in the activation energy gives agreement between the methods. From diffraction patterns and index of refraction the crystallized phase was found to be predominantly anatase.

47666 **Microstructural and Conductivity Comparison of Ag Films Grown on Amorphous TiO_2 and Polycrystalline ZnO**

R. Dannenberg, E.A. Stach, D. Glenn, P.Sieck and K. Hukari

J. Mater. Res. 2002, In Press

We report observations of significant microstructural and electrical property differences in sputtered Ag films grown on 25 nm TiO2 underlayers and amorphous TiO2 (25 nm) / ZnO (5 nm) multilayers. Transmission electron microscopy shows that the ZnO layers exhibit a strong <0001> texture, and that this texture results in a strong <111> texture in the Ag films. Ag films grown directly on TiO2 have many abnormal grains of 60 to 80 nm diameter, whereas those grown on ZnO show few abnormal grains. Additionally, the grain size the films grown on ZnO is on the order of 25 nm, while it is only on the order of 15 nm for those films deposited directly on amorphous TiO2. The Ag films grown on ZnO underlayers have sheet resistances of 5.68 W/ , whereas those grown on TiO2 have a sheet resistance of 7.56 W/ . The observed conductivity resistance is very repeatable. The improved conductivity may be a combined effect of reduced grain boundary area per unit volume, a predominance of Coincident Site Lattice boundaries with lower grain boundary resistivity and Ag planarization of the films on ZnO, resulting in less groove formation (as evidenced by atomic force microscopy observation).

Transmission Eectron Microscopy of Threading Dislocations in ZnO Films Grown on Sapphire

Sung-Hwan Lim, J. Washburn, Z. Liliental-Weber and D. Shindo

J. Vac. Sci. Tech. A 19, 2601, 2001

Threading dislocations in wurtzite ZnO films grown on the (1120) a plane of sapphire were studied by transmission electron microscopy. A majority of the threading dislocations were found to be of screw or mixed character. Dislocation half loops, elongated along the c axis, were observed. It is likely that they are formed when two screw dislocations of opposite sign attract each other during growth and combine.

49839 **Strain Relaxation and Dislocation Filtering in Metamorphic High Electron Mobility Transistor Structures Grown on GaAs substrates**

D. Lubyshev, W.K. Lieu, T.R. Steward, A.B. Cornfeld, X.M. Fang, X.Xu, P. Specht, C. Kisielowski et al

J. Vac. Sci. Tech. B 19 (4), Jul/Aug 2001

Plastic relaxation in metamorphic high electron mobility transistor (MHEMT) structures was investigated by x-ray reciprocal mapping and high-resolution transmission electron microscopy (HRTEM). X-ray data indicates that In(Ga)AlAs M buffers with a linearly graded buffer and in inverse step are completely strain compensated at the buffer-active area interface. HRTEM shows reduction of dislocation density from 109 to 106cm-2 through the M buffer. Optimized MHEMT structures were found to exhibit low rms roughness of around 2 nm and excellent electrical transport properties. MHEMT devices with 0.15 μm gates were fabricated with a transconductance of 710 mS/mm, maximum current of 500 mA/mm and gate-drain breakdown of 6.6V. A maximum ft value of 118 GHz and a maximum rf gain of 18 dB a 10 GHz were measured at a drain current of 200 mA/mm.

44900 **Magnetism and Microstructure: Imaging Techniques and Structure-Property Correlations in Information Storage Materials**

K. Krishnan

Magnetic Storage Syst. Beyond 2000, ed. G. Hadjipanayis, 251-270, 2001

Future development of ultrahigh density magnetic recording depends on developing microstructures of multicomponent and multilayered materials at the nanometer length scale. This can only be achieved by a dynamic iteration between growth of thin film structures and appropriate characterization of the physical, chemical and magnetic microstructure at relevant length scales. Electron-optic scattering, imaging and spectroscopy techniques are ideally matched to the challenge of carrying out such measurements. In this article, comprehensive reviews of the evolution of magnetic recording technology from a microstructure perspective and the status of electron microscopy based techniques are followed by examples of the application of these techniques in determining appropriate structure-property correlations. These include interface anisotropy in Co/Pt multilayers, temperature-dependent spin-reorientation transitions in c-axis oriented Co-Cr films, interface roughness and GMR in Fe/Cr multilayers and quantitative measurements of Cr-segregation and media noise in Co-Cr-Pt-X alloys.

Lorentz Transmission Electron Microscopy Investigation of Magnetically Patterned Co/Pt Multilayers

G.J. Kusinski, K.M. Krishnan, D. Weller, B.D. Terris, L. Folks, A.J. Kellock, J.E.E. Baglin and G. Thomas

Magnetic Storage Systems Beyond 2000, ed. G. Hadjipanayis, 41, 2001

The switching behavior of magnetic patterns prepared by ion irradiation was investigated. Co/Pt multilayers with perpendicular anisotropy and large out-of-plane coercivities 5-6 kOe were grown on electron transparent SiN windows. Regularly spaced 1 micron sized regions, were magnetically pattered via ion beam irradiation through a stencil mask. Lorentz TEM was used to observe in-situ magnetization reversal processes of irradiated regions under well-defined applied magnetic fields. When the in-plane field was increased, domain wall motion was observed, resulting in the alignment of the patterns with the direction of the applied field. The switching mechanism of the in-plane patterns was by domain wall motion.

49549 Shapes and Sizes of Nanoscale Pb Inclusions in Al

E. Johnson, A. Johansen, U. Dahmen, S. Chen and T. Fujii

Mat. Sc. & Eng. A 304-06, 187-93, 2001

Aluminum-lead alloys are monotectic and characterized by a large miscibility gap in the liquid phase area and extremely limited mutual solubility in the solid phase. Due to the extent of the miscibility gap the alloys are difficult to make in conventional processing. Using metastable processing techniques, it was possible to prepare alloys of aluminum with 0.5-3 at.% lead. The alloys contain fine dispersions of nanoscale lead inclusions with sizes in the range from 1 to about 20 nm after ion implantation and from 10 to 100 nm after rapid solidification. Inclusions embedded in the aluminum matrix are single crystalline, and they grow in parallel-cube alignment with the matrix. They have cuboctahedral shape with atomically smooth {111} and {100} facets determined from a minimization of the interface energy. Using high resolution TEM, two types of deviation from the classical Wulff construction which alter the shape of the inclusions, has been studied. The smallest inclusions, less than about 20 nm in size, adopt a series of magic sizes that can be related to the occurrence of periodic minima in the residual strain energy. Inclusions located in grain boundaries adopt a single crystal morphology where one part is faceted and grows in parallel-cube alignment with the matrix grain, while the other part has a shape approximating a spherical cap.

Structure and Properties of Amorphous and Nanocrystalline NiTi Prepared by Severe Plastic Deformation and Annealing

A.V.Sergueeva, C.Song, R.Z.Valiev and A.K.Mukherjee

Mat. Sci. & Eng. A 2002, In Press

The formation of homogeneous nanocrystalline structure by nanocrystallization of amorphous NiTi subjected to high pressure torsion (HPT) is demonstrated. Structural evolution during annealing was investigated and homogeneous nanocrystalline structures with different grain sizes have been obtained by controlled annealing. Nanocrystallization results in the record value of room temperature strength for this material equal to 2650 MPa with an elongation to failure of about 5%. At elevated temperatures of (0.4...0.5)Tm nanocrystalline nitinol showed a high ultimate strength with sufficient elongation (up to 200%). The observation that the shape and the size of grains after deformation remain close to that of the initial state suggests that in nanocrystalline NiTi such mechanism as grain boundary sliding and grain rotation are active and the generation and motion of dislocations play the role of accommodation of stress concentration.

Mechanical Behavior and Superplasticity of a Severe Plastic Deformation Processed Nanocrystalline Ti-6Al-4V Alloy

R.S. Mishra, V.V. Stolyarov, C. Echer, R.Z. Valiev and K. Mukherjee

Mat. Sci. & Eng. A 298, 44-50, 2001

Mechanical behavior of a sever plastic deformation (SePD) processed nanocrystalline Ti-6Al-4V alloy has been studied in the temperature range 25-675°C. Compared with the microcrystalline state, the nanocrystalline state material had higher strength up to 400°C and comparable strength above that. The ductility was significantly higher for the nanocrystalline state above 500°C, including superplasticity above 600°C. Transmission electron microscopy showed considerable grain growth and dislocation activity during superplastic deformation. A comparison of the superplastic data across the nanocrystalline and microcrystalline range showed an interesting discrepancy in the kinetics of superplastic deformation. Contrary to the general expectation, the kinetics of superplastic deformation was slower in ultrafine grained materials after normalizing the data for grain size and temperature dependence. The slower superplastic deformation kinetics in the nanocrystalline materials is discussed in terms of the difficulty associated with slip accommodation of grain boundary sliding.

Superplastic Behavior of Ultrafine-Grained Ti-6Al-4V Alloy

A.V.Sergueeva, V.V.Stolyarov, R.Z.Valiev and A.K.Mukherjee

Mat. Sci. & Eng. A 323, 318-325, 2002

Superplastic behavior of the ultrafine-grained (UFG) Ti-6Al-4V alloy produced by high pressure torsion (HPT) has been studied. High elongations (more than 500%) have been observed in this alloy during tensile tests at relatively low temperatures and high strain rates. At the same time, the superplastic behavior of this alloy has several specific features such as the relatively low values of strain rate sensitivity of flow stress and significant strain hardening. Moreover, it was shown that the alloy, processed by HPT, demonstrates an outstanding room temperature strength about 1500 MPa after superplastic deformation.

Tensile Superplasticity in Nanomaterials-Some Observations and Reflections

S.X. McFadden, A.V. Sergueeva and A.K. Mukherjee

Mat. Sci. Forum 357-359, 499-06, 2001

The synthesis of nanocrystalline materials has provided new opportunities to explore grain size dependent phenomenon to a much finer scale. Superplasticity is a well-established grain size dependent phenomenon, In this paper, we analyze some of the tensile superplasticity data obtained in the last few years on Ti-6Al-4V, Ni3Al, and 1420-Al alloy processed by severe plastic deformation (SePD). The experimental results show higher flow stresses for superplasticity in nano crystalline materials than in microcrystalline materials. It is suggested that the conventional slip accommodated grain boundary sliding is likely to be difficult in nanomaterials.

49551 **Two-Phase Lead-Tin Nanoscale Precipitates in Aluminum**

E. Johnson, A. Johansen, L. Sarholt and U. Dahmen

Mat. Sci. Forum 360-2, 267-74, 2001

Multi-component precipitates with nanoscale dimensions of elements with limited mutual solubilities can with advantage be made by sequential ion implantation. When the constituent elements of the precipitates are insoluble in the matrix, the precipitates can be considered as nanoscale ingots with the matrix acting as an array of nanoscale crucibles. Alloy precipitates of Pb-Sn embedded in an Al matrix made by sequential ion implantation have been investigated by transmission electron microscopy (TEM) and Rutherford backscattering analysis (RBS) in combination with channeling. In the as-implanted state the Pb-Sn precipitates have a cuboctahedral like shape reminiscent of the shape of pure Pb precipitates, and they have a two phase microstructure consisting of segments of Pb attached to Sn along planar interfaces close to {111}. In-situ heating and cooling experiments in the TEM show that the Sn segments in initially two-phase precipitates with off-eutectic compositions dissolve into the Pb segments below the eutectic temperature. The resulting single phase precipitates can be heavily supersaturated with Sn in comparison with the equilibrium phase diagram, and they melt in a single stage size dependent process where the largest precipitates melt first. Solidification of the precipitates takes place with little undercooling and the smallest precipitates solidify first.

49796 **Quantification of the Resolved Phase Change in Reconstructed Electron Exit Waves of Gold [110] in Different Electron Microscopes**

J. Jinschek, C. Kisielowski, M. Lentzen and K. Urban

Microscopy & Microanalysis 2002, In Press

Today material science benefits from high-resolution transmission electron microscopy (HRTEM) with a resolution that extends to the information limit of field emission microscopes into the sub Ångstrøm region. Procedures to retrieve this resolution involve a reconstruction of the complex electron exit-plane wave function by holographic recording techniques such as from focal series of HRTEM images or from single off-axis electron holograms. In this contribution we compare the recovered exit-plane phase images of electron microscopes with different contrast transfer functions (CTF) and consequentially different information limits. We tested a JEOL 3010 (LaB6), a CM200 FEG, a CM200 FEG with CS corrector [3], and a CM300 FEG/UT (OAM) [4] by taking images from the same sample of gold [110]. With this value one can extract the number of gold atoms in individual atomic columns and determine sensitivity limits that will be given.

49799 **Electron Microscopy Observations on the Role of Twinning in the Evolution of Microstructures**

U. Dahmen, C.J.D. Hetherington, V. Radmilovic, E. Johnson, S.Q. Xiao and C.P. Luo

Microscopy & Microanalysis 2002, In Press

Twinning plays an important role in phase transformations and can have significant effects on microstructural evolution. Different roles of twinning in the development of microstructures during precipitation and phase transformations are reviewed and illustrated with examples from investigations by high resolution electron microscopy, including the effect of multiple twinning on the development of Ge precipitates in Al-Ge and Ag-Ge alloys, the twin-dissociation of grain boundaries in Au, the formation of hexagonal Si at twin intersections and the effect of twin boundaries on the equilibrium shape of Pb inclusions in Al.

50092 **Quantitative Analysis of the Brownian Motion of Small Liquid Lead Inclusions in Solid Aluminum**

U. Dahmen, T. Radetic, J. Turner, S. Prokofjev, M.T. Levinsen and E. Johnson

Microscopy & Microanalysis 2002, In Press

The thermal motion of liquid inclusions or gas bubbles in solids is of fundamental and technological interest. For example, liquid migration in a thermal gradient has been used for semiconductor doping, and the rate of thermal drift indicates the mechanism of transport. Liquid Pb inclusions in Al a few nanometers, in size have been observed to undergo random motion during in-situ heating in a transmission electron microscope. The velocity and type of motion are a strong function of size and temperature. In this work, we have made direct real-time electron microscopy observations of the random motion of nanoscale liquid Pb inclusions in solid Al at temperatures around 450°C. Particle migration was recorded on video tape and analyzed frame by frame to determine the precise position of particles relative to a fixed reference frame. The resulting data sets were used to analyze the statistical properties of the particle motion and to obtain quantitative measures of the distribution of step sizes, the fractal dimension of the path of migration and the particle diffusion coefficient.

49822 **HRTEM Resolution Extension for Interface by Gerchberg-Saxton Algorithm with Supported Constraint**

F.R. Chen , U. Dahmen and J. J. Kai

Microscopy & Microanalysis 2002, In Press

High resolution TEM (HRTEM) retains distorted phases in the low spatial frequency region (less than information limit) while the information at higher spatial frequency is cut off by the lens contrast transfer function (CTF). For a medium voltage TEM, the phase information contain in a HRTEM image may only extend up to about 0.5 Å-1 , so that direct correlation of the HRTEM image of crystal structure is not trivial. The Gerchberg-Saxton algorithm has been utilized to recover the information from partial data in real and reciprocal spaces. The Gerchberg-Saxton algorithm restores spatial resolution by operating real space and reciprocal space projections cyclically.

46052 **Lighting with GaN: How Can HRTEM Help to Understand the III-Nitride System?**

C. Kisielowski, E.C. Nelson, and C. Song

Microscopy & Microanalysis 5, 822, 1999

We find that in GaN blue and green light emitting diodes an Au/Ni is used to achieve a low contact resistance. A local indium concentration of about y = 0.22 was determined at a lateral resolution of 0.5 nm. It gives rise to a green emission in a 30 nm wide well. Most surprisingly, the green emission is not caused by a large (y=0.45) indium content. A reduction of the In0.22Ga0.78N well width from 3 to 1.5 nm causes a blue shift of the initially green luminescence. Consequently, we conclude that quantum confinement and piezoelectric effects contribute largely to the light emission from these structures.

47221 **HRTEM Image Simulations of Structural Defects in Gate Oxides**

S. Taylor, J. Mardinly, M. A. O'Keefe, and R. Gronsky

Microscopy & Microanalysis 6, 1078, 2000

HRTEM is used extensively in the semiconductor industry for device characterization, and has become one of the favored techniques for characterizing the latest generation of ultra-thin gate oxides in MOSFET devices. However, relatively little is understood (either quantitatively or experimentally) about the limitations of HRTEM in detecting structural defects in gate oxides that could affect device performance.
Results from this work reveal some fundamental limitations of the utility of HRTEM for characterizing defects in gate oxides, even with the new generation of Cs corrected microscopes. These results also point out the importance of specimen preparation on the results that can be obtained.

Lorentz TEM Investigation of Magnetic Domains in Epitaxial C-Axis Oriented Co-Cr Thin Films

G.J. Kusinski

Microscopy & Microanalysis 6, 446, 2000

Continuous increase in recording densities of the Co-based longitudinal media requires a drastic scaling down of the grain size in order to keep the required signal to noise ratio. However, this approach to increase the areal density will collapse when the grain size reaches the superparamagnetic limit. As an alternative, based on the analysis of the demagnetization mechanisms, Iwasaki and Takemura suggested the possibility of perpendicular magnetic recording (PMR), and computer simulation, predict areal densities of more than 300Gbit/in2 for this configuration. The c-axis oriented Co-based hcp alloys with the magnetocrystaline anisotropy larger than the demagnetizing energy, are good candidates for the PMR media. However, before this type of materials can be realized, the magnetic domain structure must be well characterized. In this paper detailed analyses of the characteristics and shape of the magnetic domains present in the c-axis oriented CoCr films with thickness relevant for the recording industry are discussed.

47220 **HRTEM Image Simulations For Gate Oxide Metrology**

S.Taylor, J. Mardinly, M.A. O'Keefe and R.Gronsky

Microscopy & Microanalysis 6,1080, 2000

HRTEM has found extensive use in the semiconductor industry for performing device metrology and characterization. However, shrinking device dimensions (gate oxides are rapidly approaching 10Å) present challenges to the use of HRTEM for many applications, including gate oxide metrology. In this study, we performed HRTEM image simulations of a MOSFET device to examine the accuracy of HRTEM in measuring gate oxide thickness. Length measurements extracted from simulated images were compared to actual dimensions in the model structure to assess TEM accuracy. The effects of specimen tilt, thickness, objective lens defocus and coefficient of spherical abberation (C_s) on measurement accuracy were explored for nominal 10Å and 16Å gate oxide thicknesses.

49804 **Effect of Shape on Solid-Liquid Phase Changes of Xe Precipitates in an Al Matrix**

K. Mitsuishi, C.W. Allen, R. Birtcher and U. Dahmen

Microscopy & Microanalysis 7, 1258, 2001

It is well known that rare-gas Xe atoms embedded in a crystalline Al matrix form precipitates having cuboctahedral shapes bounded by {100} and {111} surfaces. Below a certain critical size, Xe precipitates are observed to be solid, even at room temperature. This is a result of the Laplace pressure, which is inversely proportional to the radius of the precipitate. Donnelly et al. reported that the critical size of Xe solidification was expected at 4nm in radius at room temperature. Using high-resolution transmission electron microscopy, it is possible to observe these particles directly. It has been demonstrated that under off-Bragg conditions, the Al lattice fringes are minimized whereas the Xe lattice fringes are maximized. From such observations, it was confirmed experimentally that the average critical size of Xe precipitates is around 4 to 5nm in radius. However, much larger Xe precipitates are sometime observed to remain solid. Such observations are in apparent contradiction to the 1/r dependence of the Laplace pressure.

HREM and Lorentz Microscopy Studies on Sm(Co, Cu, Fe, Zr)z High Temperature Permanent Magnets

Y. Zhang, W. Tang, G. Hadjipanayis, C. Chen, J. Liu, C. Nelson, K. Krishnan, Z. Luo and D. Miller

Microscopy & Microanalysis 7, 2001

Sm (Co, Cu, Fe, Zr)z 2:17 based permanent magnets have the highest Curie temperature and the most excellent temperature stability among the current rare-earth permanent magnets. In recent years, the Sm(Co, Cu, Fe, Zr)Z magnets have attracted again considerable attention due to the demand of the Department of Defense for high temperature applications such as aircraft, spacecraft and ship systems. Our recent studies have led to the development of new precipitation hardened Sm(Co, Cu, Fe, Zr)z magnets with operating temperatures above 400°C and with coercivities as high as 10kOe at 500°C. The microstructure of the Sm(Co, Cu, Fe, Zr)z high temperature magnets consists of a cellular structure (2:17 rhomobohedral cells surrounded by 1:5 hexagonal cell walls) superimposed on a lamella phase (2:17 hexagonal). This microstructure is sensitive to processing and to the alloy chemical composition. Magnetic domain structure studies play a critical role in understanding the magnetic hardening behavior of the magnets. In this paper, HREM and magnetic domain structure were studied in these Sm(Co, Cu, Fe, Zr)z high temperature permanent magnets.

49806 The Use of Moiré Patterns in TEM Images to Measure Precipitate Composition in Al-Si-Ge Alloys

V. Radmilovic, D. Mitlin, S. Hinderberger and U. Dahmen

Microscopy & Microanalysis, 7, 238, 2001

Moiré patterns are commonly formed in multiphase system when diffracting planes of similar spacing and orientation lead to interference effects. The interpretation of moiré fringes is often not straightforward due to the elastic interaction between the crystals at the interface and the dynamical nature of electron diffraction. However, if the two lattices are fully relaxed, or if a small precipitate crystal is embedded in a large matrix, moiré patterns can give a simple and direct measure of orientation and lattice constants. In the present work, the moiré technique has been applied to the quantitative analysis of lath-shaped Ge or Ge-Si precipitates in Al with the aim to determine the composition (the Si:Ge ratio) from the lattice parameter indicated by the moiré fringes.

49838 Substitutional Impurity Segregation to the Σ 5 (310)/[001] STGB in Cu Doped Aluminum and Ag Doped Copper

J.M. Plitzko, G.H. Campbell, W.E. King, S.M. Foiles and C. Kisielowski

Microscopy & Microanalysis 7, 246, 2001

The phenomenon of segregation is of long standing scientific interest and has been studied extensively, both theoretically as well as experimentally. For our investigations we have chosen the Σ 5 symmetric tilt grain boundaries (STGB) in two face-centered cubic (FCC) metals, alumnum and copper. Both metals were doped with only 1 at % of the impurity species (Cu and Ag). One of our major goals in this study was to investigate the size effect on segregation of an impurity to distinct sites at the grain boundary. Therefore we have selected the Ag as an impurity in Cu and Cu as an impurity in Al. The latter one is of special interest for applications like interconnects in microcircuits, where on of the major controlling factors of electromigration is expected to be the diffusion or segregation of Cu atoms at Al grain boundaries.

49805 **HREM Observation of the Relaxation of Grain Boundaries in Au at their Intersection with Free Surfaces**

T. Radetic and U. Dahmen

Microscopy & Microanalysis 7, 278, 2001

Thin films of gold can be grown on {001} Ge single crystal substrates in two equivalent {110} orientation variants, related to each other by a 90° rotation about the surface normal. The morphology of the films is that of a mazed bicrystal, a polycrystalline film with many randomly distributed columnar grains in only two orientations. All grain boundaries are of the type $\Sigma 99$ and display pure tilt character. In this work, we report on observations of the structural relaxation of these grain boundaries, with special emphasis on their characteristic behavior at the intersection with free surfaces and their evolution during thermal annealing.

49006 **Quantitative Investigations of Interfaces by Phase Contrast Electron Microscopy with Ultra High Resolution**

C. Kisielowski, J.M. Plitzko, S. Lartigue, T. Radetic and U. Dahmen

Microscopy & Microanalysis 7, 288, 2001

Recent progress in high resolution transmission electron microscopy makes it possible to investigate crystalline materials by phase contrast microscopy with a resolution close to the 80 pm information limit of a 300 kV field emission microscope. A reconstruction of the electron exit wave from a focal series of lattice images converts the recorded information into interpretable resolution. The present contribution illustrates some recent applications of this technique to interfaces, including the structure of heterophase interfaces between GaN and sapphire, grain boundaries in sapphire and Au, and the segregation of Cu to grain boundaries in Al.

47402 **Development of a Nanoindenter for In-Situ Transmission Electron Microscopy**

E.A. Stach, T. Freeman, A.M. Minor, D.K. Owen, J. Cumings, M.A. Wall, T. Chraska, R. Hull and J.W. Morris, Jr.

Microscopy & Microanalysis 7, 507-17, 2001

In-situ transmission electron microscopy is an established experimental technique that permits direct observation of the dynamics and mechanisms of dislocation motion and deformation behavior. In this paper, we detail the development of a novel specimen goniometer that allows real time observations of the mechanical response of materials to indentation loads. The technology of the scanning tunneling microscope is adopted to allow nanometer scale positioning of a sharp, conductive diamond tip onto the edge of an electron transparent sample. This allows application of loads to nanometer-scale material volumes coupled with simultaneous imaging of the material's response. The emphasis in this paper is qualitative and technique-oriented, with particular attention given to sample geometry and other technical requirements. Examples of the deformation of aluminum and titanium carbide as well as the fracture of silicon will be presented.

47531 **Sub-Ångstrom Transmission Electron Microscopy at 300keV**

M.A. O'Keefe, .C. Nelson, J.H. Turner and A. Thust

Microscopy & Microanalysis 7, 898, 2001

We have demonstrated sub-Ångstrom TEM to a resolution of 0.78Å with the one-Ångstrom microscope (OÅM) project at the National Center for Electron Microscopy. The OÅM combines a modified CM300FEG-UT with computer software able to generate sub-Ångstrom images from experimental image series. We achieved sub-Ångstrom resolution with the OÅM by paying close attention to detail. We placed the TEM in a favorable environment. We reduced its three-fold astigmatism A2 from 2.46μm to 300Å (corresponding to 0.68Å at a $\pi/4$ phase limit). We improved its information limit d_{Δ} by minimizing high-voltage and lens current ripple. Energy spread of 0.93eV FWHH gave a focus spread Δ of 20Å and an information limit of 0.78Å, allowing us to successfully resolve the 0.89Å (400) dumbbell spacings in [110] diamond. As a further test, we reduced the extraction voltage to 3kV to improve our information limit to 0.75Å and image 0.78Å (444) dumbbell spacings in [112] silicon as distinct pairs of "white atoms" at an alpha-null defocus of -3783Å.

Quantitative *in-situ* Nanoindentation of Thin Films in a Transmission Electron Microscope

A.M. Minor, E.A. Stach and J.W. Morris, Jr.

Microscopy & Microanalysis 7, 912, 2001

A unique *in-situ* nanoindentation stage has been and developed at the National Center for Electron Microscopy in Berkeley, CA. By using piezoceramic actuators to finely position a 3-sided boron-doped diamond indenter, we are able to image in real time the nanoindentation-induced deformation of thin films. Recent work has included the force calibration of the indenter, using silicon cantilevers to establish a relationship between the voltage applied to the piezo-actuator, the displacement of the diamond tip and the force generated. The nanoindentation of Al thin films will be discussed with relevance to phenomena such as "pop-in" behavior, dislocation nucleation and the interaction of dislocation with substrate and grain boundaries.

47532 **Alpha-Null Defocus: An Optimum Defocus Condition With Relevance For Focal-Series Reconstruction**

M. A. O'Keefe

Microscopy & Microanalysis 7, 916, 2001

Two optimum defocus conditions are useful in high-resolution transmission electron microscopy. Scherzer defocus produces an image of the specimen "projected potential" to the resolution of the microscope, and Lichte defocus minimizes dispersion. For focal-series reconstruction, alpha-null defocus maximizes transfer of high-frequency diffracted beam amplitudes. Incident-beam convergence confines beam transfer to a Gaussian "packet" of defocus values centered on the alpha-null defocus. For a diffracted beam hkl, with a spatial frequency of u, incident beam convergence has null damping effect when defocus is $-C_s\lambda^2u^2$. On either side of this alpha-null defocus value, the damping effect of incident-beam convergence reduces the diffracted-beam transfer to exp(-2), or 13.5%, when defocus reaches a value of $-C_s\lambda^2u^2.\pm \sqrt{2}/(\pi\alpha u)$. Position of alpha-null defocus for any spatial frequency depends only on the value of Cs. Defocus-packet width depends only on convergence semi-angle. Under NCEM one-Ångstrom microscope (OÅM) conditions, a [110] diamond image with correct 0.89Å spacing appears when Si (004) alpha-null defocus is selected. Alpha-null defocus should be included as the (furthest underfocus) limit for all focal series reconstruction.

Preparation and Structure of Colloidal Bimetallic Nanocrystals: The Non-Alloying System Ag/Co

N. Sobal, M. Hilgendorff, H. Möhwald, M. Giersig, M. Spasova, T. Radetic and M. Farle

Nano Lett. 2002, In Press

Monodisperse bimetallic Ag/Co-composite nanocrystals have been prepared using methods of colloid chemistry. Transmission electron microscopy showed well isolated Ag/Co-particles with a narrow size distribution centered around 10 nm in diameter. The composition of the particles was determined by energy disperse X-Ray spectrometry. Bulk like fcc-structure of both components were determined within the individual crystals using selected area electron diffraction. An AgcoreCoshell-structure of the bimetallic particles was observed by transmission electron microscopy and electron energy-loss spectroscopy.

Shape Control of CdSe Nanocrystals

X.Peng, L. Manna, W. Yang, J. Wickham, E. Scher and A. Kadavanich

Nature 404, 59-61, March, 2000

Nanometer size inorganic dots, tubes, and wires exhibit a wide range of properties1,2 that depend sensitively upon both size and shape. 3,4 In contrast to the syntheses of zero-dimensional systems, existing preparations of 1D systems often yield networks of tubes or rods, which are difficult to separate. 5-12 In the case of optically active II-VI and III-V semiconductors, the rod diameters are beyond the confinement regime. 6,8-10 Thus, except for some metal nanocrystals, 13 there are no methods of preparation that yield soluble and monodisperse 2-dimensionally quantum-confined particles. For semiconductors, a benchmark preparation is the growth of nearly spherical II-VI and III-V nanocrystals by injection of precursor molecules into a hot surfactant. 14,15 Here we demonstrate that control of the kinetics of CdSe nanocrystal growth can be used to vary the shapes of the resulting particles from a nearly spherical morphology to a rod-like one with aspect ratios as large as ten to one. The rod-like quantum confined semiconductor nanocrystals may prove advantageous in biological labeling experiments 16,17 and as chromophores in light emitting diodes (LEDs) 18,19 . Moreover, it is of considerable fundamental interest to observe their spectroscopic properties.

48818 **Structure and Properties of Co-Based Thin Films and Multilayers with Perpendicular Magnetic Anisotropy**

G.J. Kusinski

Ph.D. dissertation, U.C. Berkeley, Fall 2001

The effects of growth temperature, TG, and ion-irradiation on the magnetic properties and microstructure of Co/Pt multilayers with perpendicular anisotropy were investigated. The columnar-grain size and the <111> texture were found to increase with an increase in TG. A decrease in *HC* and domain size was measured when multilayers were exposed to ion-irradiation. The ion-induced changes in the magnetic properties are associated with a decrease in interfacial anisotropy, *KS*. Transmission electron microscopy, the ion-irradiation simulations and the calculations of interface anisotropy found the ion-induced changes of magnetic properties not to be caused by the large microstructural changes but to be associated with localized ion-beam induced atomic disordering at the Co/Pt interfaces. At high enough doses, *KS* becomes comparable to the shape anisotropy and a transition to in-plane magnetization results. The principles of ion-modification were applied to pattern the magnetic properties of the Co/Pt multilayers down to below 100 nm periodic arrays by irradiation through a stencil mask or direct focused ion beam writing. Two complementary magnetic imaging techniques were utilized: Lorentz transmission electron microscopy sensitive to in-plane magnetization and magnetic transmission x-ray microscopy sensitive to perpendicular magnetization.

50153 **High-Resolution Electron Microscopy Study of Strained Epitaxial $La_{0.7}Sr_{0.3}MnO_3$ Thin Films**

O.I. Lebedev, G. Van Tendeloo, S. Amelinckx, H. L. Ju and K.M. Krishnan

Phil. Mag. A 80, 3, 673, 2000

The microstructure of strained epitaxial $La_{0.7}Sr_{0.3}MnO_3$ (LSMO) films on a $LaAlO_3$(001) substrate has been investigated by means of electron diffraction and high-resolution electron microscopy in cross-section and plan view. Fourier transforms of the high-resolution images allow us to deduce the local lattice parameters at increasing distance from the interface. The evolution of stress in the film is studied as a function of film thickness and thermal treatment. It is found that, close to the interface, both the film and the substrate are elastically strained in the opposite sense such that the interface is perfectly coherent for thin films not exceeding a certain thickness (about 30-35nm). In thicker films, inhomogeneities develop in the as-grown films. In thicker (about 120nm) films the stress is partially relieved after annealing by the formation of coherent precipitates that contribute to the relief of stress. It is suggested that part of the mismatch strain is accommodated by the isomorphous substitution of ions of a different size and/or a different charge.

49800 **Microstructural Study of Epitaxial Platinum and Permalloy / Platinum Films Grown on (0001) Sapphire**

S. Ramanathan, B. M. Clemens and P.C. McIntyre

Phil. Mag. A 81, 2073-2094, 2001

This paper reports a detailed transmission electron microscopy study of epitaxial platinum films grown by sputtering on (0001) single crystal sapphire substrates. The orientation relationship between the platinum film and the substrate was determined to be Pt (111) || Al2O3 (0001), Pt [110] || Al2O3 [10 0]. As a result of this relationship there are two orientation variants, related to each other by 60° rotation about the [111] axis. Samples were studied in plan view and cross section to examine the morphology and faceting behavior of the grains and the atomic structure of the interfaces. Microstructural analysis using rose plots showed a large fraction (82%) of the grain boundaries oriented parallel to preferred facets along <110> directions. The films exhibited the mazed bicrystal structure, with larger grains displaying increasingly ramified shapes, a behavior that was quantified using the external form factor to describe grain morphologies. Lattice images revealed a sharp interface between the Pt and the sapphire with no intermediate phases. It is shown that the NiFe film grows as a bicrystal with the twin boundaries correlated to those of Pt. These results clearly show the importance of being able to control the microstructure of the seed layer to grow defect-free multilayers.

49552 **PVD Growth and TEM Characterization of Epitaxial Thin Metal Films on Single Crystal Si and Ge Substrates**

K. H. Westmacott, S. Hinderberger and U. Dahmen

Phil. Mag. A 81, 6, 1547-78, 2001

Epitaxial fcc, bcc and hcp metal and alloy films were grown in high vacuum by physical vapor deposition at high-rate on Si and Ge (111), (110) and (100) surfaces at different deposition temperatures. Resulting epitaxial relationships and morphological features of these films were characterized by TEM and diffraction. Simple epitaxial relationships were found mainly for the fcc metals that form binary eutectic systems with Si and Ge. Of these, Ag exhibited exceptional behavior by forming in a single crystal cube-cube relationship on all six semiconductor surfaces. Al and Au both formed bicrystal films on (100) substrates, but differed in their behavior on (111) substrates. Silicide formers such as the fcc metals Cu and Ni, as well as all bcc and hcp metals investigated, did not adopt epitaxial relationships on most semiconductor substrates. However, epitaxial single crystal, bicrystal and tricrystal films of several metals and alloys could be grown by using a Ag buffer layer. The factors controlling epitaxial growth of metal films are discussed in light of the observations and compared with predictions of established models for epitaxial relationships. It is concluded that epitaxial films can be grown easily if the film forms a simple eutectic or monotectic system with the substrate. Epitaxial relationships of those films depend on crystallographic factors for metal-metal epitaxy and on the substrate surface structure for metal-semiconductor epitaxy.

48467 Sub-Ångstrom Resolution of Atomistic Structures Below 0.8A

M.A. O'Keefe, E. C. Nelson and Y.C. Wang

Phil. Mag. B 81, 11, 1861-78, 2001

Microcharacterization of defects is greatly facilitated with improvement in resolution. By improving temporal coherence (chromatic aberration) and compensating spatial incoherence, we have achieved the goal of the 1 Å microscope (OÅM) project at the US Department of Energy's National Center for Electron Microscopy by extending the limits of high-resolution transmission electron microscopy to sub-Ångstrom levels. The OÅM combines focal-series image-processing software with a modified 300 keV electron microscope equipped with a highly coherent field emission electron gun. By operating at an 'α–null' value of underfocus in order to minimize the effects of spatial incoherence, and by reducing the OÅM's electron-gun extraction voltage to improve temporal coherence, we are able to transfer information below 0.8Å. In a test specimen of silicon viewed in the [112] orientation in the OÅM we are able to 'see' atoms separated by only 0.78Å. Sub-Ångstrom resolution at this level offers the materials researcher an effective tool for the characterization of defects with unprecedented precision.

49005 Benefits of Microscopy with Super Resolution

C. Kisielowski, E. Principe, B. Freitag and D. Hubert

Phys. B. Cond. Mat. 1090-96, 2001

TEM developed from an imaging tool into a quantitative electron beam characterization tool that locally accesses structure, chemistry, and bonding in materials with subÅ resolution. Experiments utilize coherently and incoherently scattered electrons. The interface between gallium nitride and sapphire as well as thin silicon gate oxides are studied to understand underlying physical processes and strength of the different microscopy techniques. An investigation of GaN/sapphire interface benefits largely from application of phase contrast microscopy that make it possible to visualize dislocation core structures and single columns of oxygen and nitrogen at a closest spacing of 85 pm. In contrast, it is adequate to investigate Si/SiOxNy/poly-Si interfaces with incoherently scattered electrons and electron spectroscopy because amorphous and poly crystalline materials are involved. It is shown that the SiOxNy/poly-Si interface is rougher than the Si/SiOx interface, that desirable nitrogen diffusion gradients can be introduced into the gate oxide, and that a nitridation coupled with annealing increases its physical width while reducing equivalent electrical oxide thickness to values approaching 1.2 nm. Therefore, an amorphous SiNxOy gate dielectric seems to be a suitable substitute for traditional gate oxides to increase device speed by reducing dimensions in Si technology.

50152 **Enhancement of Perpendicular and Parallel Giant Magnetoresistance with the Number of Bilayers in Fe/Cr Superlattices**

M.C. Cyrille, S. Kim, M.E. Gomez, J. Santamaria, K.M. Krishnan and I.K. Schuller

Phys. Rev. B 62, 2000

We have correlated a detailed quantitative structural analysis by X-Ray diffraction, TEM and high spatial electron energy loss spectroscopy (EELS) imaging, with the magnetization and anisotropic magnetotransport properties in sputtered Fe/Cr supperlattices. To accomplish this, we developed a technique for magnetotransport measurements in metallic superlattices with the current perpendicular to the plane of the layers (CPP). Using microfabrication techniques, we have fabricated microstructured Fe/Cr pillars embedded in SiO2 and interconnected with Nb electrodes and the minimization of the superlattice-electrode contact resistance, the method allows a simple and independent measurement of the superlattice resistance and GMR. Structural and magnetic characterization of [Fe(3nm)/Cr(1.2n]n superlattices (where N is the number of repetitions) indicate that the roughness is correlated and increases cumulatively through the superlattice stack with no significant change in the AF coupling. Both the current in plane (CIP) and CPP GMR increase with N as the roughness increases.

Effects of Structural Defects on the Activation of Sulfur Donors in GaNxAs1-x Formed by N Implantation

J. Jasinski, K. M. Yu, W. Walukiewicz, Z. Liliental-Weber and J. Washburn

Physica B 308-310, 874, 2001

The effects of structural defects on the electrical activity of S-doped GaNxAs1-x layers formed by S and N co-implantation in GaAs are reported. S and N ions were implanted to the depth of about 0.4 mm. Electrochemical capacitance voltage measurements on samples annealed at 945°C for 10 s show that in a thin (<0.1 mm) surface layer the concentration of active shallow donors is almost an order of magnitude larger in S and N co-implanted samples than in samples implanted with S alone. The activation efficiency of S donors also shows a broad minimum at a depth of about 0.2 mm below the surface. The results of these electrical measurements are correlated with the distribution of structural defects revealed by transmission electron microscopy (TEM). The TEM micrographs show that in addition to a band of dislocation loops commonly found in ion implanted GaAs, an additional band of small voids is observed in samples co-implanted with S and N. The location of this band correlates well with the region of reduced electrical activation of S donors, suggesting that the formation of the voids through N accumulation results in a lower concentration of "active", substitutional N atoms.

Polarity of GaN Grown on Sapphire by Molecular Beam Epitaxy with Different Buffer Layers

D. Huang, P. Visconti , F. Yun, M. A. Reshchikov, T. King, A. A. Baski, C. W. Litton, J. Jasinski, Z. Liliental-Weber and H. Morkoç

Physica Status Solidi a 188, 571, 2001

We report on the polarity of GaN films grown on sapphire substrates by molecular beam epitaxy using different buffer layers and growth conditions. On high temperature AlN or GaN buffer layers, the GaN films typically show Ga or N-polarity, respectively. When low temperature (either AlN or GaN) buffer layers are employed, GaN films of both polarities can be grown, but these films have a high density of inversion domains. Insertion of additional GaN/AlN quantum dot layers between the buffer layers and the GaN films provides strain relief and a significant improvement in the quality of the GaN epilayers.

Influence of Dopants on Defect Formation in GaN

Z. Lilinetal-Weber, J. Jasinski, I. Grzegory, and S. Porowski, D.J.H. Lambert, C.J. Eiting, and R.D. Dupuis

Physica Status Solidi b 228, 345, 2001

The influence of p-dopants (Mg and Be) on the structure of GaN has been studied using Transmission Electron Microscopy (TEM). Bulk GaN: Mg and GaN: Be crystals grown by a high pressure and high temperature process and GaN: Mg grown by metal-organic chemical-vapor deposition (MOCVD) have been studied. A structural dependence on growth polarity was observed in the bulk crystals. Spontaneous ordering in bulk GaN: Mg on c-plane (formation of Mg-rich planar defects with characteristics of inversion domains) was observed for growth in the N to Ga polar direction (N polarity). On the opposite side of the crystal (growth in the Ga to N polar direction) Mg-rich pyramidal defects empty inside (pinholes) were observed. Both these defects were also observed in MOCVD grown crystals. Pyramidal defects were also observed in the bulk GaN: Be crystals.

Investigation of Defects and Polarity in GaN Using Hot Wet Etching, Atomic Force and Transmission Electron Microscopy and Convergent Beam Electron Diffraction

P. Visconti, F. Yun, D. Huang, K. M. Jones, M. A. Reshchikov, R. Cingolani and H. Morkoç, J. Jasinski et al

Physica Status Solidi b 228, 513, 2001

Availability of reliable and quick methods to investigate defects and polarity in GaN films is of great interest. We have used photo-electrochemical (PEC) and hot wet etching to determine the defect density. We found the density of whiskers formed by the PEC process to be similar to the density of hexagonal pits formed by wet etching and to the dislocation density obtained by transmission electron microscopy (TEM). Hot wet etching was used also to investigate the polarity of MBE-grown GaN films together with convergent beam electron diffraction (CBED) and atomic force microscopy (AFM). We have found that hot H3PO4 etches N-polarity GaN films very quickly resulting in the complete removal or a drastic change of surface morphology. On the contrary, the acid attacks only the defect sites in Ga-polar films leaving the defect-free GaN intact and the morphology unchanged. The polarity assignments, confirmed by CBED experiments, were related to the as-grown surface morphology and to the growth conditions.

A Comparative Study of MBE-Grown GaN Films Having Predominantly Ga- or N-Polarity

F. Yun, D. Huang, M. A. Reshchikov, T. King, A. A. Baski, W. Litton, J. Jasinski, Z. Liliental-Weber and H. Morkoç

Physica Status Solidi b 228, 543, 2001

Wurtzitic GaN epilayers having both Ga and N-polarity were grown by reactive molecular beam epitaxy using a plasma-activated nitrogen source on c-plane sapphire. The polarities were verified by convergent beam electron diffraction. High-resolution X-ray diffraction, atomic force microscopy imaging and transmission electron microscopy were employed to characterize the structural defects present in the films. The different topographic features of Ga and N-polarity samples and their appearance after wet etching were correlated to the measured X-ray rocking curve peak widths for both symmetric [0002] and asymmetric [1014] diffraction. For Ga-polarity samples, the [0002] diffraction is narrower than the [1014] diffraction, while for N-polarity ones the [0002] peaks are broader than [1014]. The half width of [1014] peaks for both polarity types were in the range of 5-7 arcmin indicative of a high density of pure edge threading dislocations lying parallel to the c-axis. The 1-2 arcmin [0002] linewidths of Ga-polarity samples suggest a low density of screw dislocations. In N-polarity samples, however, the [0002] diffraction peak was typically wider than 5 arcmin, suggesting either a higher density of edge dislocations and inversion domains.

Correlation Between Deformation Mechanisms and Microstructural Evlution in Silicon Nitride Ceramics

J.A. Schneider and A.K. Mukherjee

Precursor-Derived Ceram., Synth. Struct. & High Temp. Mech. Prop, ed. J. Bill, F. Wakai, F. Aldinger, Wiley-VCH, 270-279, 1999

Changes of phase composition and morphology were investigated in silicon nitride both before and after compressive deformation testing. Si3Ni4 specimens have been consolidated that retained the equiaxed, metastable α-phase. Use of additives such as MgAl2O4 promote formation of a high viscosity additive system which rapidly pull the grains together by capillary forces during the liquid phase sintering prior to the phase transformation. If additives are used such as Y2O3 which promote formation of a low viscosity additive phase, the phase transformation from α to β–phase occurs prior to completion of the liquid phase sintering resulting in elongated grains. Equiaxed initial structures of the α-phase are noted to transform to an equiaxed β–phase microstructure following the elevated temperature compression tests. A recent model has proposed an interface control mechanism that may be correlated with enhanced deformation in Si3Ni4. These studies are in agreement with this model and indicate an equiaxed morphology is required to permit grain rearrangement in response to applied stress.

48466 **Sub-Ångstrom Transmission Electron Microscopy for Materials Science**

M.A. O'Keefe, E.C. Nelson and U. Dahmen

Proc. 9th Int'l BCEIA C-UFEMMS A81, 2001

High-resolution electron microscopy (HREM) is becoming even more important as materials scientists build artificially-structured nano-materials. Nanostructures often include atoms with bond lengths shorter in projection than the point resolution of a standard mid-voltage HREM. Image simulations show that structure determination of defects such as dislocation cores need sub-Ångstrom resolution. Sub-Ångstrom TEM is also important for atomic-level analysis of interface structure and for tomographic reconstruction of 3-dimensional shapes of nanocrystals. Research on embedded nanocrystals show that this knowledge is essential for understanding of magic-size behavior recently found from Pb inclusions in Al. Similar needs arise in the characterization of nanoscale dynamic phenomena such as size-dependent phase separation, superheating or premelting in small particles or inclusions.

49176 HRTEM Image Simulations of Structural Defects in Gate Oxides

S. Taylor, J. Mardinly, M. A. O'Keefe and R. Gronsky

Proc. AIP #550, 2001

In this study, we performed HRTEM image simulations of a MOSFET device to determine the ability of HRTEM to detect gate oxide defects. The gate oxide was modeled as an amorphous silicon oxide 16.3 Å thick, sandwiched between a gate and substrate. Both the gate and substrate were modeled as (100) silicon viewed along the [110] direction. Crystalline silicon defects were embedded in the model gate oxide and simulated images were calculated using a multi-slice approach with varying defect morphology, composition. size and orientation. Simulations predict that defects should be observable for very small specimen thickness (<100Å) and large defect sizes (>40Å), but not for specimen thickness and defect sizes typical of advanced CMOS devices analyzed in routine electron microscopy.

49166 HRTEM Image Simulations For Gate Oxide Metrology

S.Taylor, J. Mardinly, M.A. O'Keefe and R.Gronsky

Proc. AIP #550, 2001

In this study, we performed HRTEM image simulations of a MOSFET device to evaluate the accuracy of HRTEM in measuring gate oxide thickness. Gate oxide thickness measurements extracted from simulated images were compared to actual dimensions in the model structure to assess TEM accuracy. Results reveal no consistent trends in measurement accuracy as a function of specimen thickness, specimen thickness, specimen tilt, or objective lens defocus. In general, thickness measurements performed with conventional TEM could not be determined reliably with precision better than 10%. However, thickness measurements could be maede with no error using a spherical aberration corrected TEM.

Magnetic Reversals in Ion-Beam Nano-Patterned Co/Pt Multilayers

G.J. Kusinski, K.M. Krishnan, G. Thomas, G. Denbeaux, D. Weller and B.D. Terris

Proc. APS 2001, In Press

Cobalt/Platinum multilayers with perpendicular magnetic anisotropy, were patterned into magnetic arrays by ion irradiation. The irradiated regions show change of the easy axis of magnetization from out-of-plane to in-plane. The magnetic reversal processes of two types of magnetic arrays, (a) in-plane magnetized dots surrounded by out-of plane matrix and (b) of out-of-plane dots surrounded by in-plane matrix, were studied. Two complementary magnetic imaging techniques were utilized. Lorentz transmission electron microscopy, sensitive to the in-plane magnetization, revealed magnetically soft ion-irradiated areas. The x-ray transmission microscope at the ALS, utilizing contrast due to magnetic circular dichroism (MCD) at the Co L3 absorption edge, was used to image perpendicular magnetization. The imaged patterns showed decrease in intensity for irradiated regions due to change of the easy axis of magnetization from out-of-plane to in-plane. The same area imaged off the Co edge, showed no contrast indicating no topographical changes and only magnetic patterning. For the irradiated samples the reversal originated at the edges of irradiated regions and propagated into the non-irradiated surroundings. These results are correlated with the physical microstructure, which was investigated using conventional, high resolution and energy filtered transmission electron microscopy

Investigation of Surface Polarity in GaN Using Hot Wet Etching Together with Reflection High Energy Electron and Convergent Beam Electron Diffraction

P. Visconti, D. Huang, K. M. Jones, M. A. Reshchikov, F. Yun, A.A. Baski, T. King, H. Morkoç, J. Jasinski , W. Swider, et al.

Proc. E-MRS Spring Meeting H-III.3, 2001

The availability of reliable and quick methods to determine defect density and polarity in GaN films is of great interest. We have used photo-electrochemical (PEC) and hot wet etching using H3PO4 and molten KOH to estimate the defect density in GaN films grown by hydride vapor phase epitaxy (HVPE) and molecular beam epitaxy (MBE). Free-standing whiskers and hexagonal etch pits are formed by PEC and wet etching respectively. Using Atomic Force Microscopy (AFM), we found the whisker density to be similar to etch pit densities for samples etched under precise conditions. Additionally TEM observations confirmed dislocation densities obtained by etching which increased our confidence in the consistency of methods used. Hot wet etching was used also to investigate the polarity of GaN films together with Convergent Beam Electron Diffraction and AFM imaging. We found that hot H3PO4 etches N-polarity GaN films very quickly resulting in the complete removal or drastic change of surface morphology as revealed by AFM or optical microscopy. On the contrary, the acid attacks only defect sites in Ga-polarity films producing nanometer-scale pits but leaving the defect-free GaN intact and the morphology unchanged. Additionally, the polarity assignments were related to the as-grown morphology and to the growth conditions of the buffer layer and the subsequent GaN layer.

49526 High Resolution TEM Observation of CVD Diamond Films

A.G. Fitzgerald, Y. Fan, C.Kisielowski, P. John, C.E. Troupe, J.I.B. Wilson

Proc. EMAG 168, 39, 2001

High Resolution Electron Microscopy has been used to study the microstructure of CVD diamond films. The lattice image observations show that the predominant structural defects in the diamond films are microtwins and stacking faults. The majority of the twin crystals have a laminar structure with $\Sigma 3$ coherent boundaries. In addition, some high order non coherent twin boundaries are also observed n the five-fold symmetry twinned diamond crystals.

50082 Clustering and Precipitation in Al-Si-Ge and Al-Si-Ge-Cu Alloys

V. Radmilovic, U. Dahmen, B. Dracup, M.K. Miller, D. Mitlin and J.W. Morris

Proc. ICAA-8, Cambridge UK, 2-5 July 2002, In Press

Atom probe tomography and high resolution electron microscopy revealed that in the very early stage of aging Al-Si-Ge alloys, clustering of Si and Ge atoms takes place followed by precipitation at structural defects. Electron microscopy observations demonstrated that precipitates are multiply twinned throughout the aging treatment. Any twinned section of the precipitate no longer maintains low-index interfaces with the matrix, and consequently goes from a crystallographic to a spherical interface with the matrix. This explains the equiaxed shape of the Si-Ge precipitates. CALPHAD calculation predicted and X-ray microanalysis confirmed a decreasing concentration of Ge within the equilibrium precipitate as the aging temperature is increased. In the quaternary Al-Si-Ge-Cu alloy, Si-Ge particles quickly nucleate and grow during elevated temperature aging. The Si-Ge particles then act as nucleation sites for θ' precipitates, resulting in a peak aged microstructure consisting of a dense distribution of θ' attached to Si-Ge.

41595 Microstructural Characteristics of Rapidly Quenched $Nd_2Fe_{14}B/\alpha$-Fe Exchange-Spring Magnets

M. Benaissa, K. Krishnan and V. Panchanathan

Proc. ICEM 14, 553, 1998

Due to their high value of maximum energy product, (BH)max, rapidly quenched Nd-Fe-B alloys based on the ternary $Nd_2Fe_{14}B$ phase are considered the cornerstone of a new class of high performance permanent (or hard) magnets. Although these permanent magnets are characterized by large magnetocrystalline anisotropy, they suffer from a low saturation magnetization with respect to soft magnetic materials such as iron. To overcome this limitation, a combination of magnetically soft and hard phases with a well defined ideal microstructure and a strong magnetic exchange coupling was proposed. This exchange-spring mechanism is supposed to permit no easy mechanism of irreversible magnetization reversal in either of the two phases. The future development of more powerful magnets is determined by our ability to understand and control intrinsic properties such as the microstructure of these composite permanent magnets. In this study we emphasize the influence of chemical composition variation on the microstructure, and its impact on the coercivity mechanism and remanence of rapidly quenched Nb-doped $Nd_2Fe_{14}B$ /α–Fe composites.

49678 Dislocation Core in GaN

Z. Liliental-Weber, J. Jasinski, J. Washburn and M. A. O'Keefe

Proc. ICEM-15 2002, In Press

Light emitting diodes and blue laser diodes grown on GaN have been demonstrated despite six orders of magnitude higher dislocation density than that for III-V arsenide and phosphide diodes. Understanding and determination of dislocation cores in GaN is crucial since both theoretical and experimental work are somewhat contradictory. Transmission Electron Microscopy (TEM) has been applied to study the layers grown by hydride vapor-phase epitaxy (HVPE) and molecular beam that voids are formed along the dislocation line in HVPE material, the dislocations have closed cores. Similar results of closed core are obtained for the screw dislocation in the MBE material, confirming earlier studies.

49808 **HREM, Z-Contrast and Atomistic Modelling: A Quantitative Study on the Sigma5 (310)/[001] Boundary in Cu Doped Al**

J. M. Plitzko, C. Kisielowski, G. Duscher, G. Campbell, W. King and S. Foiles

Proc. ICEM-15 2002, In Press

To determine the atomistic structure at the Σ5 (310)/[001] symmetric tilt grain boundary (STGB) in copper doped (1 a %) aluminum we used HRTEM in combination with focal-series reconstruction (FSR), Z-contrast imaging and theoretical ab-initio calculations. Nowadays, field emission microscopes are widely spread and very popular because of their advantages over thermionic emitters (high brightness, very coherent electron beam, etc.). However, the interpretation of HRTEM images obtained with field emission sources is not straightforward because the image is a highly encoded mixture out of TEM and object properties. To overcome this, we can use FSR of the exit wave function to exclude the imaging artifacts. Additionally, FSR can provide not only detailed information on the atomic structure but also chemical information related to the projected potential (Z=atomic number) of the elements under investigation.

49679 **Experiences with Remote Electron Microscopy**

M. O'Keefe and B. Parvin

Proc. ICEM-15 2002, In Press

With the advent of a rapidly proliferating international computer network, it became feasible to consider remote operation of instrumentation normally operated locally. For modern electron microscopes, the growing automation and computer control of many instrumental operations facilitated the task of providing remote operation. In order to provide use of NCEM TEMs by distant users, a project was instituted in 1995 to place a unique instrument, a Kratos EM-1500 operating at 1.5 MeV, on-line for remote use. In 1996, the Materials Microcharacterization Collaboratory (MMC) was created as a pilot project within the US Department of Energy's DOE2000 program to establish national collaboratories to provide access via the Internet to unique or expensive DOE research facilities as well as to expertise for remote collaboration, experimentation, production, software development, modeling, and measurement. A major LBNL contribution to the MMC was construction of Deep View, a microscope-independent computer-control system that could be ported to other MMC members to provide a common graphical user-interface (GUI) for control of any MMC instrument over the wide area network

49677 **Measurement of the Electron Beam Energy-Spread Contribution to Information Transfer Limits in HRTEM**

M. A. O'Keefe, P. Tiemeijer and M. Sidorov

Proc. ICEM-15 2002, In Press

Sub-Angstrom TEM of materials at intermediate voltages requires a sub-Angstrom information limit for the microscope. With a Scherzer resolution of 1.7A, but a sub-Angstrom information limit, the one-Angstrom microscope (OAM) project at the NCEM is able to generate resolution below 0.8A. Microscope information limit comes from damping of transfer by the temporal coherence. A major term contributing to temporal coherence is energy spread in the electron beam. We derive a new expression for the energy spread, and show how it can be measured from the result that is obtained using a standard electron spectrometer.

49795 **Exit Wave Reconstruction, Cs Correction, Z-Contrast Microscopy: Comparative Strengths and Limitations**

C. Kisielowski, J. Jinschek, K. Mitsuishi, U. Dahmen, M. Lentzen, J. Rignalda and T. Fliervoet

Proc. ICEM-15 2002, In Press

Currently available electron microscopes are at the threshold of routine operation with sub Angstrom spatial resolution together with around 100 meV energy resolution. Moreover, theory and experiment merge on this scale since computational abilities have improved to a point where materials properties can be predicted from computer models that contain a similar number of atoms as those observable by high resolution TEM. To benefit fully from this unique development it is crucial to develop a methodology that is capable of comparing quantitatively the strengths and limitations of different microscopes and emerging techniques such as exit wave reconstruction, Z-contrast imaging and Cs correction. In a series of experiments on gold [110] and silicon [110] quantitative data about sensitivities, precision, and resolution of these techniques were produced and will be reported.

49797 **The Stability of Double Slab Configuration for Two-Phase Inclusions**

K. Mitsuishi, D. Chatain, E. Johnson, K. Furuya and U. Dahmen

Proc. ICEM-15 2002, In Press

Transmission electron microscopy allows the direct observation of nano-scale particles embedded in a solid matrix, revealing their size, shape, crystal structure and internal substructure. As a result it is now possible to study the stability of the various configurations of two-phase particles embedded in a third phase, and to compare experimental observations with theoretical predictions. For example, the eutectic phase separaton in Pb-Cd nanosize particles embedded in an Al matrix has been studied by in-situ electron microscopy during melting, solidification and alloying by ion implantation. Although generally, particles were found to be composed of two segments, one from each phase, joined along a single planar interface, particles with two or multiple slabs have also been observed. Such double slab configurations have been considered metastable because the additional interface area is expected increase the energy. In the present work, the stability of the double slab configuration of two-phase systems confined in a third phases is studied for the two-dimensional case of a hexagonal shape.

50095 **Resolution Extension for Structural Multiplicity in Σ=5 (210) TiO_2 Grain Boundary Using Gerchberg-Saxton Indirect Microscopy**

Fu-Rong Chen , U. Dahmen and J. J. Kai

Proc. ICEM-15 2002, In Press

At least eight degrees of freedom are needed to describe the atomic structure of grain boundaries. To distinguish between different atomic structures in boundaries that are macroscopically identical requires accurate local measurement of rigid shifts and clear distinction between different structural units. To analyze structural units at grain boundaries in compounds such as ceramic oxides, HRTEM must have sufficient resolving power to distinguish different types of atoms. In the current work, we have employed the Gerchberg-Saxton algorithm to extend the HRTEM resolution of a Σ=5 (210) grain boundary in TiO2.

50063 Structure –Property Relations in Pt-Mo Electrocatalysts

V. Radmilovic, N. Markovic and P. Ross

Proc., ICEM-15 2002, In Press

Pt-based electrocatalysts used in fuel cells are usually multimetallic particles dispersed on a high area carbon black support. Electron microscopy (EM) techniques are used to determine the uniformity of the spatial distribution of the metallic particles, the particle size distribution, and as much about the microstructure of individual particles as possible, e.g. shape, twinning, facetting, and composition. EM techniques are especially useful for microcharacterization of electrocatalysts because they are, by necessity, electronically conducting. These analyses can provide an adequate, although not necessary complete characterization of the microstructure of the catalyst that we could use to correlate the surface activity of Pt-Mo nanoparticles with the model bulk PtxMoy alloy surfaces. The catalytic properties of the electrocatalysts are then correlated to the microstucture of the particles, aided by the kinetic studies of model systems such as Pt(hkl) single crystals and bulk alloys.

50081 TEM and CALPHAD Assisted Aluminum Alloy. Design

V. Radmilobic, U. Dahmen, B. Dracup, P. Turchi and J.W. Morris

Proc. ICEM-15 2002, In Press

Aluminum based alloys are materials of choice for future aerospace and automotive applications. However, despite extensive work on these alloys, the principles underlying their physical properties are still not fully understood, and alloy design has been mostly empirical. In this work, we combine structural and chemical characterization by transmission electron microscopy with computer phase diagram calculation to develop a systematic understanding of the relationship between microstructure and properties and to aid in the design of a new Al-Cu-Si-Ge alloy.

50094 HREM Observations of Interfaces In Gold

C.J.D. Hetherington, A.I. Kirkland, R.R. Meyer, J.L. Hutchison and U. Dahmen

Proc. ICEM-15 2002, In Press

Gold bicrystal {111} films, prepared using Ge surfaces as a template have been observed in recent years in a variety of transmission electron microscopes. The specimens are ideal for TEM studies as they may be made easily, are not fragile and the films are uniformly thin over large areas with a high density of edge-on boundaries. They are also a challenge to the high resolution electron microscopist since the spacing of the gold {220} planes, at 0.144nm, lies beyond the point-to-point resolution limits of most conventional TEMs. These "standard" specimens allow a comparison of the various approaches to higher resolution electron microscopy that are now emerging.

50091 Random Thermal Migration of Small Liquid Lead Inclusions in Solid Aluminum

U. Dahmen, T. Radetic, J. Turner, S. Prokofjev, M.T. Levinsen and E. Johnson

Proc. ICEM-15 2002, In Press

Nanometer-size Pb inclusions in Al exhibit a number of interesting phenomena that depend strongly on size and shape. For example, nanoscale solid Pb inclusions in Al are cuboctahedral in shape, bounded by {111} facets and truncated on {100} facets, and particles tend follow a sequence of magic sizes. It has also been shown that before melting, Pb particles superheat by an amount that is in inverse proportion to their size. The smallest particles can superheat by as much as 100°C. Upon further heating, migration of the liquid inclusions has been observed at rates that are directly recordable using in-situ TEM. The velocity and type of motion are a strong function of size and temperature. Particle migration was recorded on video tape at constant temperature and subsequently analyzed frame by frame. The resulting data sets were used to analyze the statistical properties of particle motion, to measure the distribution of step sizes and to determine nature of the inclusion trajectory.

50093 **TEM Observations on the Role of Twinning in the Evolution of Microstructures**

U. Dahmen, C.J.D. Hetherington, V. Radmilovic, E. Johnson, S.Q. Xiao and C.P. Luo

Proc. ICEM-15 2002, In Press

Twins and stacking faults are commonly observed during crystal growth and phase transformations in materials with low stacking fault energy. Often, these features occur on the scale of a few interatomic distances, and they are directly related to local morphology and defect structure. High resolution phase contrast microscopy has played an important role in the analysis of twins and stacking faults because it provides a direct view of the crystal lattice, its orientation relationship with neighboring regions, its disruption by defects and interfaces, and its correlation with morphology. By relating local twin or defect structures with shape it has been possible to elucidate the role of twinning in the evolution of precipitates in Al-Ge and Ag-Ge alloys.

50090 **Quantitative HREM Analysis of a Constrained $\Sigma 3$ {112} Grain Boundary in Au**

Dahmen, J.M. Penisson, R. Kilaas and D. Medlin

Proc. ICEM-15 2002, In Press

The structure of elastically constrained short segments of the incoherent $\Sigma 3$ {112} twin boundary in gold was studied by high resolution electron microscopy (HREM). Such boundaries were found at the ends of narrow microtwins, forming the connecting segments that join two long parallel {111} coherent twin boundaries. Several such boundaries of different length were studied and compared with atomistic simulations using quantitative techniques.

49812 **Real Time Observations of Dislocation-Mediated Plasticity in the Epitaxial Al (110) / Si (001) Thin Film System**

E.A. Stach and W.D. Nix

Proc. ICSMA 2001, In Press

Despite numerous theoretical and experimental studies of strain relaxation in metal films on silicon substrates, the exact mechanisms by which dislocations mediate plasticity in these structures are not well understood. To elucidate these mechanisms, we present results from *in-situ* TEM annealing of aluminum films grown on Si (001). As a model system, we have chosen to focus on epitaxial aluminum films grown by physical vapor deposition (PVD) on Si at 280 C. This growth technique results in the creation of a bicrystalline film with two variants of Al (110) oriented grains (Thangaraj, et al. APL 1992). Following an initial annealing step at 450 C to promote grain growth, the materials are thermal cycled between 450 C and room temperature within the objective lens of the microscope. This allows real time observation of the evolution of the dislocation array in response to thermal strains. Our preliminary observations show that during cooling, pre-existing dislocations move relatively slowly and appear to move parallel the (110) plane of the film. At the tensile yield point, however, dislocation motion along the standard (111) 1/2 [110] slip systems occurs in a burst, and subsequent glide along the (111) planes during further cooling is hindered by dislocation interactions. As the sample continues to cool, additional bursts of glide are observed which permit dislocations to overcome these obstacles.

In-situ LTEM Investigations of Switching of the Magnetic Patterns Prepared by Ion-Beam Irradiation

G.J. Kusinski, D. Weller, B.D. Terris, L. Folks, A.J. Kellock, C. Rettner, J.E.E Baglin, M.E. Best and K.M.Krishnan

Proc. MRS 2000, In Press

The Co/Pt multilayers with perpendicular anisotropy were grown on electron transparent Si_3N_4 membranes using electron beam evaporation. Regularly spaced 1 micron sized regions, with the easy axis of magnetization rotated into the plane of the film, were magnetically pattered via ion beam irradiation through a silicon stencil mask. Typical conditions were 700 keV nitrogen ions at doses of 5-10x1015cm-2. Transmission electron microscope analysis revealed no microstructural or chemical differences between the irradiated and non-irradiated regions. A wide log-normal grain size distribution, with approximately a 50nm mean diameter, was observed. In-situ magnetizing experiments, in which magnetization reversal processes were viewed directly in the presence of varying magnetic fields, were staged in the transmission electron microscope operated in the Lorentz mode. In the remanent state the in-plane areas supported a multidomain configuration with the domain size in the order of 350nm. When the in-plane filed component was increased to 200Öe, domain wall motion was observed, resulting in alignment of the patterns with the direction of the applied field. The significant softening of the in plane regions as compared to the out of plane coercivity, (HC = 5-6kÖe) was confirmed by Kerr measurements of larger, 4x4mm areas exposed to the same doses of ion radiation.

Mechanism for Ion Beam Modification of Magnetic Properties of Thin Films and Multilayers

J.E.E. Baglin, D. Weller, L. Folks, M. Toney, A.J. Kellock, B.D.Terris, E. Fullerton, S. Maat, C.T. Rettner and G.J. Kusinski

Proc. MRS 2000, In Press

We have investigated the physical mechanism whereby ion irradiation produces large changes in the magnetic properties of thin films suitable for magnetic recording, e.g. [Co/Pt] multi-layers, or Fe-Pt alloy films. These effects are the basis of ion beam patterning techniques proposed for future high density storage. Samples were irradiated with He, N, Ar or Xe ions at energies between 30 keV and 1 MeV, with doses spanning the range 10e14- 5e16 ion/cm2. We then examined the dependence of the magnetic properties on ion energy, species and dose, and on the media structure, (number and thickness of layers; stoichiometry). Structural characterization was done using AFM, MFM, LTEM, XRR, RBS, and ion channeling. We attribute the magnetic effects primarily to short-range chemical disordering effects at multilayer interfaces or within alloy media, induced by ion beam mixing. The model appears to be supported by TRIM simulations.

49817 **Structure Refinement of S-Phase Precipitates in Al-Cu-Mg Alloys by Quantitative HRTEM**

R. Kilaas, V. Radmilovic and U. Dahmen

Proc. MRS 2000, In Press

The crystal structure of the Al_2CuMg S-phase in an Al matrix has been determined by quantitative high resolution electron microscopy. This work combines techniques of image processing and quantitative comparison between experimental and simulated images with automatic refinement of imaging and structural parameters.

Reversal Processes in Ion-irradiation Patterned Co/Pt Multilayers

G.J. Kusinski, Kannan M. Krishnan, G. Thomas, G. Denbeaux, B.D. Terris and D. Weller

Proc. MRS 2001, In Press

(111) textured (Co0.3nm/Pt1nm)10 multilayers with perpendicular anisotropy were grown on electron transparent SiN windows using electron beam evaporation. These multilayers were patterned into magnetic sub-micron arrays by ion beam irradiation through a stencil mask and by a direct Ga Focused Ion Beam writing. Two complementary electron and photon magnetic imaging techniques were utilized to study the reversal processes of the patterned magnetic arrays. Lorentz transmission electron microscopy, sensitive to the in-plane magnetization, revealed magnetically soft ion-irradiated areas. X-ray transmission microscope at the Advanced Light Source, utilizing element specificity (Co L3 absorption edge) and magnetic contrast due to magnetic circular dichroism (MCD), was used to image the reversal of perpendicular magnetization with a 25 nanometer resolution. Reversing the applied field direction resulted in partial switching of the un-irradiated areas at fields below the sample coercivity (HC^ = 6.3kOe). The reversal originated at the edges of the patterns and propagated into the non-irradiated surrounding regions. Details of the magnetizing experiment including the reversal mechanism for the samples exposed to different irradiation doses are discussed in the paper.

Relaxation of Grain Boundaries in Au {110} Bicrystal Thin Films Observed by HREM

T. Radetic and U. Dahmen

Proc. MRS 2001, In Press

Thin films of gold can be grown on {001} Ge single crystal substrates in two equivalent {110} orientation variants, related to each other by a 90° rotation about the surface normal. The morphology of the films is
that of a mazed bicrystal, a polycrystalline film with many randomly distributed columnar grains in only two orientations. All grain boundaries are of the type S99 and display pure tilt character. In this work, we report on observations of the structural relaxation of these grain boundaries, with special emphasis on their characteristic behavior at the intersection with free surfaces and their evolution during thermal annealing.

Characterization of Very Low Defect-Density Free-Standing GaN Substrate Grown by Hydride-Vapor-Phase-Epitaxy

P. Visconti, M. A. Reshchikov, K. M. Jones, F. Yun, R. Cingolani, and H. Morkoç, J.Jasinski, W. Swider, Z. Liliental-Weber et al

Proc. MRS 680, 2001, In Press

Structural, electrical and optical properties of free-standing 200-mm thick GaN films grown by hydride vapor phase epitaxy (HVPE) have been investigated. After laserlift-off, the GaN substrates were mechanically polished on both Ga and N-sides and dry etched only on the Ga-side to obtain a smooth epi-ready surface. Hot H3PO4 chemical etching on both surfaces was used to reveal the defect sites, which appeared as hexagonal pits. The etched surfaces were then examined by atomic force microscopy. A few seconds of etching was sufficient to smooth the N-face surface and produce etch pits with a density of ~$1x10^7$ cm^{-2}. In contrast, a 50 minute etching was needed to delineate the defect sites on the Ga-face which led to a density as low as $5x10^5$ cm^{-2}. From plan-view and cross-sectional transmission electron microscopy (TEM) analysis, we have estimated that the dislocation density is less than about $5x10^6$ cm^{-2} and ~$3x10^7$ cm^{-2} for the Ga and N-faces respectively. Hall measurements demonstrated very high mobility (1100 and 6800 cm^2 /Vs at 295 and 50 K, respectively) and very low concentration of donors ($2.1x10^{16}$ cm^{-3}) and acceptors ($4.9x10^{15}$ cm^{-3}). In the photoluminescence (PL) spectrum taken at 10 K, a rich excitonic structure has been observed with the highest peak attributed to the exciton bound to neutral shallow donor (BDE).

A Method for Extracting Quantitative Data During *In Situ* Nanoindentation

A.M. Minor, E.T. Lilleodden, E.A. Stach, and J.W. Morris, Jr.

Proc. MRS 695, 2001, In Press

The development of a novel transmission electron microscope holder has made real time observations of nanoindentation possible. Using a piezo-ceramic loading mechanism, a diamond indenter is pushed into the surface of a sample, while the electron beam images the deforming sample in cross section. In this paper, we present the method for calibrating the force-displacement- voltage relation and load-frame compliance associated with this instrument. This allows quantitative force-displacement measurements to be obtained, in the manner of traditional indentation experiments. As an example of the utility of this technique, we present observations of the indentation behavior of an Al thin film on silicon, which have been previously shown [1]. Indentation into a coarse grain shows a displacement excursion corresponding to the nucleation of dislocations, and is compared to force-displacement responses measured with instrumented indentation techniques.

What Xe Nanocrystals in Al Can Teach Us in Materials Science

C. W. Allen, R.C. Birtcher, U. Dahmen, K. Furuya, M. Song and S. E. Donnelly

Proc. MRS 703, 463-68, 2002

Noble gases are generally very insoluble in solids. For example, Xe implanted into Al at 300 K forms a fine dispersion of crystalline precipitates and, at large enough fluence, fluid precipitates, both of which are stabilized, relative to the gas phase, by the Laplace pressure due to precipitate/matrix interface tensions. High resolution electron microscopy has been performed to determine the largest Xe nanocrystalline precipitate in local equilibrium with fluid Xe precipitates within the Al matrix. From the shape and size of the largest crystal and the Laplace pressure associated with its interface, we show that the interface tensions can be derived by setting the Laplace pressure equal to the pressure for solid/fluid Xe equilibrium derived from bulk Xe compression isotherms at the temperature of equilibration and observation. The Xe/Al interface tensions thus derived are in the range of accepted values of surface tensions for the Al matrix. Furthermore, it is suggested that this same technique may be employed to estimate unknown surface tensions of a solid matrix from the size and shape of maximal nanocrystals of a noble gas element, which have been equilibrated in that matrix at the temperature of observation.

49798 **Quantitative HRTEM Investigation of an Obtuse Dislocation Reaction with a Cs Corrected Microscope**

J. Jinschek, C. Kisielowski, T. Radetic, U. Dahmen, M. Lentzen, A. Thust and K. Urban

Proc. MRS Spring, 2002, In Press

We utilized a CM200 FEG instrument equipped with a Cs corrector to investigate quantitatively the core structure of an obtuse dislocation reaction in gold. A determination of the structure from a single lattice image is compared with the result from an exit wave reconstruction. Quantitative information is obtained by extraction of the column positions surrounding the dislocation core with precision on a pm level. Moreover, it is shown that the large scattering power of the gold atoms (atomic number Z=79) can be utilized to extract the number of gold atoms in individual atomic columns from reconstructed electron exit-waves of wedge shaped samples. A comparison of multi-slice calculations with experiments gives guidelines on how resolution affects the limit as to which the number of atoms in a particular column can be determined from a phase change of the electron exit wave. Since the magnitude of the phase change oscillates with sample thickness and depends on resolution, it is principally possible to probe the information limit of an electron microscope through the maximum phase change.

49801 **The Core Structure of a 30° Partial Dislocation in GaAs: Merging Theory and Experiment Quantitatively**

X. Xu, P. Specht, E.R. Weber, S.F. Beckman, D.C. Chrzan and C. Kisielowski

Proc. MRS Spring, 2002, In Press

In recent years it became possible to extent the resolution of field emission microscopes into the sub Angstrom region by reconstruction of the electron exit wave from a focal series of lattice images. Thereby, it is now feasible to investigate defects and interfaces on a truly atomic scale in many materials systems. On the other hand, progress in theory enables scientists to calculate the total energy configuration of systems that are comparable in size with what is typically investigated by high-resolution transmission electron microscopy. Therefore, a quantitative investigation of the agreement between theoretical calculations and experiments is feasible. In this contribution we investigate the core structure of a 30-degree partial dislocation in low temperature grown GaAs:Be. Ab initio electronic structure total energy calculations are used to compute the expected structure for both the Ga-centered and the As-centered 30 degree partial dislocation cores in GaAs..

Structure and Magnetism of Co and CoAg Nanocrystals

M. Spasova, T. Radetic, N. Sobal, M. Hilgendorff, U. Wiedwald, M. Farle, M. Giersig and U. Dahmen

Proc. MRS Spring, 2002, In Press

Monodisperse, air-stable Co (11.4 nm diameter, size deviation $s < 5\%$) and CoAg55 (11 nm diameter, < 10%) nanoparticles have been prepared using methods of colloidal chemistry. High resolution transmission electron microscopy and Electron Energy-Loss Spectroscopy element-specific TEM images reveal a multiply-twinned fcc Co metallic core covered with a 2-2.5 nm thick CoO shell. The lattice parameters are close to the ones of bulk Co and CoO. A shift of the hysteresis loop of 0.4 T, induced by field cooling of the Co/CoO particles, indicates strong unidirectional exchange anisotropy due to the interaction between the ferromagnetic Co core and the antiferromagnetic CoO shell. CoAg55 composite particles consist of grains of fcc Co and fcc Ag. No evidence for alloy formation was observed. EELS images indicate that Co is predominantly found in the surface region of the particles. SQUID magnetometry shows that at room temperature the CoAg55 particles are superparamagnetic while at 90 K a hysteresis loop was detected with the coercive field of 0.07 T and a remanent magnetisation of 32 % of the saturation value.

45345 **The Microstructure and Properties of Al-Si-Ge-Cu Alloys**

D. Mitlin, V. Radmilovic, U. Dahmen and J.W. Morris

Proc. Termec Las Vegas, 2000

It has been known for some time that alloying Al with a combination of Si and Ge produces a moderately dense distribution of fine, compact precipitates. For this reason, the Al-Si-Ge system has been proposed as a possible source of thermally stable Al alloys with moderate strength. A reinvestigation of aging behavior in this alloy system shows, however, that it is difficult to achieve precipitate densities that are high enough to make a meaningful contribution to the strength. On the other hand, a Si-Ge addition can be used to provide a dense template of heterogeneous nucleation sites for subsequent precipitation of Al-Cu precipitates. We have used this approach to process Al-Si-Ge-Cu alloys to have excellent combinations of strength and thermal stability in the aged condition.

Creep of Silicon Nitride/Silicon Carbide Ceramic Nanocomposites

M.J. Gasch, J. Wan, K.C. Lieu, E.Lara-Curzio and K. Mukherjee

Proc. TMS 247-55, 2002

In comparison to conventional ceramic sintering techniques, polymer precursors offer new methods for making silicon nitride/silicon carbide ceramic composites with microstructural features not attainable by hot pressing. Pyrolsis-derived amorphous powders prepared either by iron(Fe) or tungsten carbide (WC) ball milling where Electric Field Assisted Sintered (EFAS), with 8% Y2O3 as an additive, in 10 minutes at 1600°C. Sintering of such powders results in microstructures with a matrix of 100-200nm silicon nitride grains amongst nanometric silicon carbide grains and a small amount of residual amorphous phase. Depending on powder processing method, high temperature mechanical testing of consolidated specimens exhibit creep rates of 3.5 x 10--9 s-1 at 1400°C and 100Mpa. The rate parameters for creep were established from mechanical tests. Microstructures, prior to and post creep testing, were examined with TEM in order to shed light on the rate controlling creep mechanisms.

50087 **Ordering in a Fluid Inert Gas Confined by Flat Surfaces**

S. Donnelly, R. Birtcher, C. Allen, I. Morrison, K. Furuya, M. Song, K. Mitsuishi and U. Dahmen

Science 296, 507-10, 2002

High-resolution transmission electron microscopy images of room-temperature fluid xenon in small faceted cavities in aluminum reveal the presence of three well-defined layers within the fluid at each facet. Such interfacial layering of simple liquids has been theoretically predicted, but observational evidence has been ambiguous. Molecular dynamics simulations indicate that the density variation induced by the layering will cause xenon, confined to an approximately cubic cavity of volume 8 cubic nanometers, to condense into the body-centered cubic phase, differing from the face-centered cubic phase of both bulk solid xenon and solid xenon confined in somewhat larger (20 cubic nanometer) tetradecahedral cavities in face-centered cubic metals. Layering at the liquid-solid interface plays an important role in determining physical properties as diverse as the rheological behavior of two-dimensionally confined liquids and the dynamics of crystal growth.

Advanced Mechanical Properties Of Pure Titanium With Ultrafine Grained Structure

A.V.Sergueeva, V.V. Stolyarov, R.Z.Valiev and A.K.Mukherjeea

Scripta Mat. 45 747-752, 2001

The mechanical properties of CP Ti at room temperature were investigated. The decreasing grain size in CP Ti leads to significant increases in its hardness and/or strength. A combination of SPD by HPT at 5 GPa followed by short annealing at low temperatures allows one to obtain a high strength (more than 1200 MPa) in pure material that is comparable in strength to alloyed Ti.

46053 **Strain in GaN Thin Film and Heterostructures**

C. Kisielowski

Semiconductors and Semimetals 57 Academic Press, 275-317,1999

This paper reviews our current understanding of stress and strain related phenomena in GaN thin films and heterostructures. It focuses on the impact of strain on thin film growth though almost any physical property of the GaN thin films is affected by stress and strain. Some examples will be given which concern the surface morphology of GaN films, the native doping concentration and the luminescence. Quantitative high resolution TEM is used to investigate alloy fluctuations in barrier and well structures.

Dislocation-Independent Mobility in Lattice-Mismatched Epitaxy, Application to GaN

D.C. Look, C.E. Stutz, R.J. Molnar, K. Saarinen and Z. Liliental-Weber

Solid State Communications 117, 571, 2001

Lattice-mismatched epitaxy produces a high concentration of dislocations (Ndis) in the interface region, and this region is often highly conductive, due to donor (ND) decoration of the dislocations. Here we show that a simple postulate, ND= a (Ndis/c), where c is the lattice constant and a a constant of order 1-2, predicts a nearly constant low-temperature mobility, independent of Ndis. This prediction is experimentally verified in GaN grown on Al2O3, and is also applied to other mismatched systems.

Properties and Microstructure of Alumina-Niobium Nanocomposites Made by Novel Processing Methods

J.D Kuntz, J. Wan, G. Zhan and A.K. Mukherjee

Ultrafine Grained Materials II, TMS 225-233, 2002

Alumina-niobium nanocomposites have been fabricated using high-energy ball milling and electric field assisted sintering(EFAS) or high pressure sintering (HPS). The 10 volume percent niobium nanocomposites have fracture toughnesses greater than 6 MPa$\sqrt{m}$ with only a marginal decrease in hardness. This is nearly twice as tough as a pressureless sintered composite of the same composition reported in work by Garcia et al [1]. This increase in toughness can be attributed to the novel microstructure in the nanocomposites. The present study shows a metallic phase distribution of ~20nm particles along with a continuous 3-4 nm layer at boundaries between alumina grains. This microstructure should lead to toughening by increasing ductility at the crack tip instead of the traditional ligament bridging in the crack wake which is typical of micron-scaled metallic-phase toughened ceramics.

Nano-Nano Composites of Silicon Nitride and Silicon Carbide

J.Wan, M.J. Gasch and A.K. Mukherjee

Ultrafine Grained Materials II, TMS 235-244, 2002

This is an effort of bringing the grain size scale of silicon nitride and silicon carbide composites into the truly nanometric range, i.e., with the grain size of both silicon nitride and silicon carbide within 100 nm limit. Amorphous Si-C-N bulk materials were first synthesized by a processing route based on pyrolysis of polymer precursor. By controlling the crystallization heat-treatment at relatively low temeperature levels, and without oxide sintering additives (thus no liquid phase to promote grain growth), silicon nitride/silicon carbide composites with grain size of 30-50 nm can be achieved. The phase ratio of silicon nitride versus silicon carbide in the composites can readily be controlled by an ammonia-treatment at certain stage of the processing of amorphous ceramics. Detailed TEM investigation revealed that dual-grain junctions (grain boundaries) are free of oxide glassy phases, which are often present in conventionally sintered ceramics. However, small amount of residual Si-C-N amorphous phase can be found at multi-junctions of the grains.

48245 **Structure Determination and Structure Refinement of Al_2CuMg Precipitates by Quantitative High Resolution Electron Microscopy**

R. Kilaas and V. Radmilovic

Ultramicroscopy 88, 63 2001

The structure of the S-Phase (Al_2CuMg) precipitate in an Al matrix has been determined by using a combination of image processing, quantitative image comparison between experimental and theoretical images, and automatic refinement of imaging and structural parameters. A method for comparing images with unknown origin relationship while quickly estimating a possible translation of the origin is outlined. The optimization algorithm used in the structure determination utilizes space group symmetries, which are deduced from the crystal zone axis, and reduces the number of free parameters.

47046 **Sub-Ångstrom High-Resolution Transmission Electron Microscopy at 300keV**

M.A. O'Keefe, C.J.D. Hetherington, Y.C. Wang, E.C. Nelson, C. Kisielowski, J.H. Turner J.-O. Malm, R. Mueller, et al

Ultramicroscopy 89, 215-41, 2001

Sub-Ångstrom transmission electron microscopy with an interpretable resolution of about 0.8Å has been achieved at the NCEM for the first time. The NCEM one-Ångstrom microscope (OÅM) project is designed to provide materials scientists with transmission electron microscopy at a resolution significantly better than one Ångstrom. To achieve this resolution, the OÅM uses extensive image reconstruction to exploit the substantially higher information limit of a specially-modified FEG-TEM over its Scherzer resolution limit. Reconstruction methods include off-axis holograms or focal series of underfocused images. The NCEM OÅM is the first TEM designed to have its information limit extended by hardware correction of three-fold astigmatism and improved electrical stability of the microscope high voltage and objective lens current. Although modifications to the OÅM were designed to produce an information limit of 0.82Å, measured values of coherence parameters predict an information limit of 0.78Å and this limit is confirmed experimentally. The resolution enhancement of the OÅM results from its improved electrical stability coupled with focal series reconstruction to its information limit, effectively making its spherical aberration (coefficient of 0.6mm) irrelevant.

47162 **Imaging Columns Of the Light Elements Carbon, Nitrogen and Oxygen with Sub Ångstrom Resolution**

C. Kisielowski, C.J.D. Hetherington, Y.C. Wang, R. Kilaas, M.A. O'Keefe and A. Thust

Ultramicroscopy 89, 243-63, 2001

It is reported that lattice imaging with a 300 kV field emission microscope in combination with numerical reconstruction procedures can be used to reach an interpretable resolution of about 80 pm for the first time. A retrieval of the electron exit wave from focal series allows for the resolution of single atomic columns of the light elements carbon, nitrogen, and oxygen at a projected nearest neighbor spacing down to 85 pm. Lens aberrations are corrected on-line during the experiment and by hardware such that resulting image distortions are below 80 pm. Consequently, the imaging can be aberration-free to this extent. The resolution enhancement results from increased electrical and mechanical stability's of the instrument coupled with a low spherical aberration coefficient of 0.595 + 0.005 mm.

National Center for Electron Microscopy
Lawrence Berkeley National Laboratory
One Cyclotron Road
M/S 72-150
Berkeley, California 94720

National Center for Electron Microscopy
Lawrence Berkeley National Laboratory
One Cyclotron Road
M/S 72-150
Berkeley, California 94720

Please send a reprint of the paper(s):

Number	First Author	Title (first two words)

Name_____ Date_____

Affiliation _____

Address _____

_____

Please send a reprint of the paper(s):

Number	First Author	Title (first two words)

Name_____ Date_____

Affiliation _____

Address _____

_____

☆U.S. GOVERNMENT PRINTING OFFICE: 2002-784-682

National Center for Electron Microscopy
Ernest Orlando Lawrence
Berkeley National Laboratory
University of California
Berkeley, CA 94720